Aus der Anatomischen Anstalt der Ludwig-Maximilians-Universität München

Lehrstuhl I-vegetative Anatomie

Vorstand: Prof. Dr. med. Jens Waschke

Identification of motoneurons innervating individual extraocular muscles within the oculomotor nucleus in human

Dissertation zum Erwerb des Doktorgrades der Medizin

an der Medizinischen Fakultät

der Ludwig-Maximilians-Universität zu München

vorgelegt von

Emmanuel Che Ngwa

aus

Kumba, Cameroon

Jahr

2016

Mit Genehmigung der Medizinischen Fakultät

der Universität

Berichterstatter:	Prof. Dr. J.A. Büttner-Ennever Ph.D
Mitberichterstatter:	Priv. Doz. Dr. Roger Kalla
	Priv. Doz. Dr. Sandra Becker-Bense
Mitbetreuung durch die promovierte Mitarbeiterin:	Prof. Dr. rer. nat. A. Horn-Bochtler
Dekan:	Prof. Dr. med. dent. Reinhard Hickel

TAG DER MÜNDLICHEN PRÜFUNG:

30.06.2016

Table of contents

Table of figures

Abbreviations

AM:	anteromedian nucleus
BSA:	bovine serum albumin
CCN:	central caudal nucleus
CEN:	central subgroup in nIII
ChAT:	choline acetyltransferase
CMRF:	central mesencephalic reticular formation
CR:	calretinin
DL:	dorsolateral subgroup in nIII
DM:	dorsomedial subgroup in nIII
EW:	Edinger-Westphal nucleus
EWcp:	central projecting part of EW
EWpg:	preganglionic neurons of EW
GABA:	gamma amino butyric acid
GAD:	glutamate decarboxylase
INC:	interstitial nucleus of Cajal
IO:	inferior oblique muscle
IR:	inferior rectus muscle
LAT:	lateral subgroup in nIII
MIF:	multiply-innervated muscle fibre
MLF:	medial longitudinal fascicle
MR:	medial rectus muscle
nIII:	oculomotor nucleus
nIV:	trochlear nucleus
nVI:	abducens nucleus
NP-NF:	non-phosphorylated neurofilaments
PBS:	phosphate buffer solution (pH 7.4)
RIMLF:	rostral interstitial nucleus of the medial longitudinal fascicle
RT:	room temperature
C:	motoneurons of multiply-innervated fibres of IR and MR
S:	motoneurons of multiply-innervated fibres of IO and SR
SIF:	singly-innervated muscle fibre
SO:	superior oblique muscle
SR:	superior rectus muscle

TBS: tris buffered saline

UCN: urocortin

VEN: ventral subgroup in nIII

ABSTRACT

The oculomotor nucleus (nIII) and trochlear nucleus (nIV) of the midbrain contain motoneurons that innervate extraocular eye muscles. The aim of this study is to identify the motoneuronal subgroups of the human nIII and nIV, which innervate individual extraocular muscles using several histochemical stains, and comparing the results with those obtained in monkey. The nIV innervates only the superior oblique (SO) muscle, whereas nIII contains extraocular motoneurons, which innervate the medial rectus (MR), inferior rectus (IR), superior rectus (SR) and inferior oblique (IO) muscles. The organization of the motoneuron subgroups in human is not clear, and is the main subject of this investigation. In monkey the localization of the motoneuron subgroups for individual muscles is well known as a result of tract tracing studies, and analyses of their differential transmitter inputs. The results in monkey provided a useful basis for this study on human nIII.

Human brainstems were fixed in 4% paraformaldehyde, series of frozen and paraffin sections of 40µm, 10µm and 5µm respectively were stained with choline acetyltransferase (ChAT) antibody to identify cholinergic motoneurons of extraocular muscles. The ChAT sections were then immunostained for the inhibitory transmitter GABA with antibodies against glutamate decarboxylase (GAD) or for the calcium-binding protein calretinin (CR). The cytoarchitecture of nIII was visualized with cresyl violet, gallyas stain or antibodies against non-phosphorylated neurofilaments (NP-NF).

Six subgroups were delineated in nIII: a dorsolateral (DL), dorsomedial (DM), central (CEN), ventral (VEN), lateral group (LAT) and the nucleus of Perlia (NP), in addition to the central caudal nucleus (CCN) and the urocortin-positive centrally projecting neurons of the Edinger-Westphal nucleus (EWcp). The DL, VEN, LAT, EWcp and NP groups receive a strong supply of GAD-positive terminals as the SO motoneurons in nIV. Strong CR-immunoreactivity was found in the CEN group, NP and CCN, but not in nIV.

Based on the staining properties of the subgroups and a comparison to the existing studies on monkey nIII, the CCN was considered to innervate the levator palpebrae; the CEN group was identified as the upgaze motoneuron subgroup for SR and IO, and DL, VEN and LAT showed characteristics of MR motoneurons. For the first time two separate subgroups of motoneurons (DL and VEN) subserving motor pathways for MR were identified in the human nIII,

whereby the DL subgroup corresponds to the B-group and the VEN subgroup to the A-group in the monkey nIII. The DM group was considered to innervate IR muscle. The strong CR input to NP revealed characteristics of upgaze motoneurons in nIII. A good correlation was found between monkey and human in CR stains. But surprisingly, there were striking differences between monkey and human nIII with GAD stains. The results indicate that human MR motoneurons may contribute to a specialized function, e.g. during vergence, by its strong GABAergic input.

ZUSAMMENFASSUNG

Der Nucleus oculomotorius nIII und Nucleus trochlearis (nIV) im Mittelhirn enthalten die Motoneurone der extraoculären Augenmuskeln. Ziel der vorliegenden Arbeit war die Identifizierung der verschiedenen Motoneuronengruppen im humanen nIII und nIV, welche individuelle Augenmuskeln innervieren. Dies erfolgte anhand verschiedener histochemischer Färbungen, die im Vergleich zu Daten an Affen erhoben wurden. Der nIV innerviert nur den Musculus obliquus superior (SO), während nIII die Motoneurone von Musculus rectus medialis (MR), inferior (IR), superior (SR) und Musculus obliquus inferior (IO) enthält. Die Organisation der Motoneuronengruppen im Menschen ist noch nicht eindeutig geklärt und ist Hauptthema der vorliegenden Studie. Im Affen ist die Lokalisation der einzelnen Motoneuronengruppen individueller Augenmuskeln aufgrund von Trakt-Tracer-Studien etabliert, ebenso wie die Transmittereingänge zu den einzelnen Gruppen, die als Basis für die vorliegende Arbeit am menschlichen nIII dienten.

Humane Hirnstämme wurden in 4% Paraformaldehyd fixiert, und Serien von Gefrier- und Paraffinschnitten (40µm, 10µm und 5µm) wurden mit Antikörpern gegen Cholinacetyltransferase (ChAT) gefärbt, um die cholinergen Motoneurone der äußeren Augenmuskeln zu identifizieren. Die auf ChAT angefärbten Schnitte wurden dann mit einer weiteren Immun-Peroxidase-Färbung auf den inhibitorischen Transmitter GABA mit Antikörpern gegen Glutatmatdecarboxylase (GAD) oder das Calcium-bindende Protein Calretinin (CR) angefärbt. Die Zytoarchitektur des nIII wurde mit einer Kresyl-Violett-Färbung, Gallyas-Färbung oder Immunfärbung auf nicht-phosphorylierte Neurofilamente (NF-NP) dargestellt.

Sechs Untergruppen konnten im nIII des Menschen voneinander abgegrenzt warden: eine dorsolaterale (DL), dorsomediale (DM), zentrale (CEN), ventrale (VEN), laterale Gruppe (LAT) neben dem Nucleus Perlia (NP) und dem Nucleus centralis caudalis (CCN) und der urocortin-positiven central projizierenden Neurone des Edinger-Westphal Kerns (EWcp). Die Gruppen DL, VEN, LAT, EWcp and NP erhalten einen starken Eingang von GAD-positiven Endigungen, ebenso die Motoneurone des SO im nIV. Eine starke Immunreaktivität für CR wurde innerhalb des nIII nur in der CEN-Gruppe gefunden, sowie dem NP und CCN, nicht aber im nIV.

Basierend auf den histochemischen Eigenschaften der einzelnen Motoneuron-Subgruppen im Affen wurde beim Menschen der CCN bestätigt als der Kern, der die Motoneurone des Musculus levator palpebrae enthält; die CEN-Gruppe wurde anhand der selektiven CR-Eingänge als Sitz der Motoneurone von SR und IO identifiziert, die Blickbewegungen nach oben bewirken. Die Gruppen DL, VEN und LAT zeigten die Eigenschaften von MR-Motoneuronen, die DM-Gruppe die von IR-Motoneuronen. Hierbei konnte zum ersten mal gezeigt werden, dass auch beim Menschen der MR in zwei Gruppen innerhalb des nIII repräsentiert ist, wobei DL der B-Gruppe, und VEN der A-Gruppe beim Affen entspricht. Ein weiterer neuer Befund zeigte sich für den NP, der einen starken CR-Eingang erhält und damit eher Eigenschaften von Motoneuronen für Aufwärtsblick (wie SR und IO) aufweist. Insgesamt fand sich eine gute Übereinstimmung in den histochemischen Eigenschaften der Motoneuroneingänge bezüglich CR zwischen Mensch und Affe. Aber überraschenderweise war beim Menschen ein viel stärkerer GAD-Eingang auf die Motoneurone für horizontale Augenbewegungen (MR) als beim Affen präsent. Diese Daten weisen auf eine spezialisierte Rolle der MR-Motoneurone im Menschen, z.B. bei Vergenz, hin.

1 INTRODUCTION

1.1 EXTRAOCULAR EYE MUSCLES

Vertebrates possess six extraocular muscles, five of which originate from the annulus of Zinn surrounding the optic nerve. These are the superior rectus (SR), inferior rectus (IR), lateral rectus (LR), medial rectus (MR) and superior oblique (SO) muscles (Fig. 1). The inferior oblique (IO) muscle has its origin from the lacrimal fossa located in the nasal portion of the orbit (Fig. 1). In mammals an additional eye muscle, the levator palpebrae muscle (LP), which elevates the upper eyelid originates from the annulus of Zinn as well and inserts on the superior palpebra (for review: Spencer and Porter, 2006). Embryologically the extrinsic eye muscles develop in a caudo-rostral pattern. MR, IR, SR and IO originate from cells in the rostral anlage (premandibular), the SO from cells in the middle anlage (mandibular) and lateral rectus from cells in the caudal anlage (hyoid). The mammalian LP develops from the premandibular anlage (Porter and Baker, 1992; Spencer and Porter, 2006) and is a derivate of the superior rectus muscle (SR) (Siebeck and Kruger, 1955; Isomura, 1981).

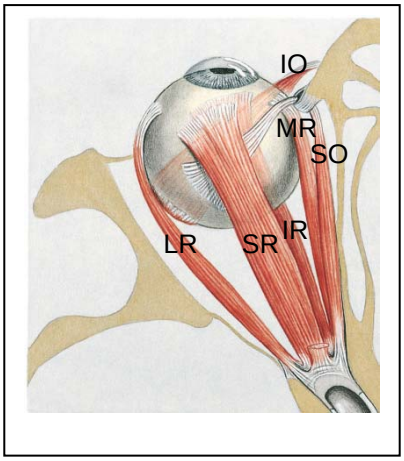

Figure 1. Dorsal view of the left human orbita
The eye is moved by six extraocular muscles: this includes four recti muscles: the medial rectus (MR), inferior rectus (IR), superior rectus (SR) and lateral rectus muscle (LR) and 2 oblique muscles: inferior oblique (IO) and superior oblique muscle (SO).
With permission from Elsevier. Adopted from: Paulsen, Waschke, Sobotta Atlas der Anatomie des Menschens, 23.Auflage 2010 © Elsevier GmbH, Urban & Fischer, München (Abb. 9.39 modified).

1.2 MOTOINNERVATION OF EXTRAOCULAR MUSCLES AND EYE MOVEMENTS

The innervation of the extraocular eye muscles is highly consistent through all vertebrates (Büttner-Ennever 2006). Coordination of motion is initiated due to nerval innervation from motoneurons in the oculomotor, trochlear (nIV) or abducens nuclei (nVI). The MR, IR, IO are innervated by motoneurons from the ipsilateral nIII, those of the SR from the contralateral nIII. The SO and the LR are innervated from the nIV and nVI respectively (Büttner-Ennever, 2006). Studies in frontal-eyed animals including primates demonstrate that a midline group of motoneurons lying between the nIII and nIV, called the central caudal nucleus (CCN), innervates the levator palpebrae muscle (LP), bilaterally (Porter et al., 1989; Schmidtke and Büttner-Ennever, 1992; Van der Werf et al., 1997).

Depending on origin, insertion and their muscle paths the extraocular muscles can move the eyes in all directions (Fig. 2) (Leigh and Zee, 2015). For the horizontal plane MR and LR function in an antagonistic fashion with each other whereas for vertical eye movements IO and SR move the eye upward, SO and IR move the eye downward, rotatory eye movements are achieved by different combinatory actions of these muscles (Tab. 1). In primates at least five different types of eye movements are distinguished from each other that provide inputs to the motoneurons by anatomically separated premotor pathways. These are saccades, the vestibulo-ocular reflex, optokinetic reflex, smooth pursuit eye movements and convergence (Horn and Adamcyzk, 2011). Lesions of the oculomotor nucleus may lead to deficits such as squint, diplopia and pupillary abnormalities (Leigh and Zee, 2015).

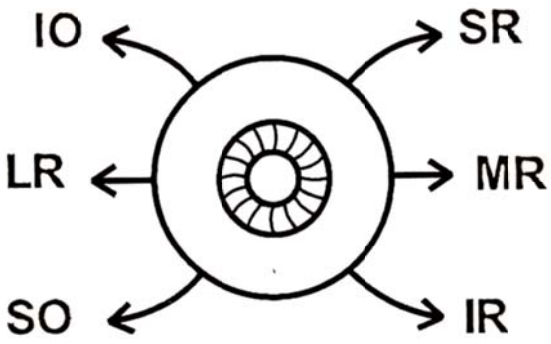

Figure 2. Diagram of pulling directions of the extraocular muscles
The arrows indicate the pulling directions of the extraocular muscles for the right eye.

Eye muscle	Insertion	Function
MR	Sclera of eyeball, nasally	Adduction
SR	Sclera of eyeball, rostral	Adduction, elevation, intorsion
IR	Sclera of eyeball, caudal	Abduction, depression, extorsion
LR	Sclera of eyeball, laterally	Abduction
SO	Sclera of eyeball, rostral	Abduction, depression, intorsion
IO	Sclera of eyeball, caudal	Abduction, elevation, extorsion
LP	Levator palpebrae	Elevation of the upper eyelid

Tab.1 Overview of extraocular eye muscles with their insertion points and function.
MR, medialis rectus; SR, superior rectus; IR, inferior rectus; LR, lateral rectus; SO, superior oblique; IO, inferior oblique; LP, levator palpebrae;

1.2.1 THE LOCATION AND STRUCTURE OF THE TROCHLEAR NUCLEUS

The trochlear nucleus (nIV) is located in the tegmentum of the midbrain at the level of the colliculus inferior. At caudal planes the nIV is partially embedded in the fibres of the medial longitudinal fascicle (MLF) (Büttner-Ennever and Horn, 2014).
The nIV consists of motoneurons supplying mainly the contralateral SO (Warwick 1953, Büttner-Ennever, 2006), whereas in rabbits a small population (3%) of small-sized neurons provide an ipsilateral projection (Murphy et al., 1986). In monkey a dorsal cap of nIV smaller motoneurons is located that supply the multiply-innervated slow non-twitch muscle fibers of the superior oblique muscle (Büttner-Ennever et al., 2001). A similar population of motoneurons is present in human as well (Büttner-Ennever and Horn, 2014).

1.2.2. EXPERIMENTAL STUDIES OF THE TROCHLEAR NUCLEI

The cytoarchitecture of nIV has been studied in different species of vertebrates such as amphibians (Naujoks-Manteuffel et al. 1986; Muñoz and González, 1995), reptiles (El-Hassni, 2000), birds (Sohal et al., 1985), and mammals including rabbits (Murphy et al., 1986), mouse (Sturrock, 1991), monkeys (Büttner-Ennever et al. 2001) and rats (Glicksman,

1980). The morphology of the human nIV was studied in adults (Zaki, 1960; Büttner-Ennever and Horn, 2014) and at fetal stages (Pearson, 1943; Cooper, 1946; 1947). Morphometric studies on adult human trochlear nucleus revealed 1500 motoneurons in one study (Zaki, 1960) and between 1810 and 2400 in another study (Vijayashankar and Brody 1977). The latter number remains relatively constant based on studies from 20 male brains at various postnatal ages.

1.2.3. THE LOCATION AND STRUCTURE OF THE OCULOMOTOR NUCLEUS

The oculomotor nucleus (nIII) is also located in the midbrain tegmentum and adjoins the nIV rostrally. Pearson and coworkers described the development of nIII in human and divided it into three parts (Pearson, 1944). Based on studies in amphibians it was found that the motoneurons of nIII develop from the mesomere, found in the most caudal part of the midbrain (Matesz, 1990; Baker, 1992; Straka et al., 1998; Straka et al., 2001).

Based on Nissl stainings in transverse human midbrain sections, the caudal part of nIII is round or oval in shape and lies dorsal and dorsomedial to the MLF. At caudal planes through nIII the unpaired central caudal nucleus is located between the dorsal aspects of both nIII (Schmidtke and Büttner-Ennever, 1992; Horn and Adamczyk, 2011; Büttner-Ennever and Horn, 2014). At more rostral planes through nIII, the midportion of the nucleus is almost triangularly shaped with both halves separated from each other by the nucleus of Perlia (NP) (Perlia, 1889). At the dorsal border of nIII a compact small-celled nucleus appears, which is now termed the centrally projecting part of the Edinger-Westphal nucleus (EWcp) (see section 1.4) (for review: Kozicz et al., 2011). At rostral planes through nIII, the EWcp adjoins the dorsal, ventral and rostral border and merges with the unpaired anteromedian nucleus (Büttner-Ennever and Horn, 2014).

The nIII is composed of multipolar neurons with pronounced Nissl substance, similar to those of the trochlear and abducens nuclei, which show characteristic features of motoneurons. The oculomotor complex contains motoneurons that innervate the *ipsilateral* medial rectus, inferior rectus, inferior oblique and the *contralateral* superior rectus; and about 36% of the oculomotor nerve fibers from the caudal oculomotor nucleus arise from the contralateral side and cross the midline within the nucleus (Büttner-Ennever and Horn, 2014).

1.2.4 EXPERIMENTAL STUDIES OF OCULOMOTOR SUBGROUPS IN MONKEYS

1.2.4.1. Degeneration methods

Since the 18th century, many studies on the topographical arrangement of motoneurons within the nIII have been done in several vertebrate species (for review: Evinger, 1988; Büttner-Ennever, 2006). In monkeys especially, fundamental experimental studies progress arising from clinical observations and the use of retrograde degeneration methods (Von Gudden, 1881). The rostro-caudal and dorso-ventral arrangement of functional subgroups by Bender and Weinstein (1943) was acknowledged and elaborated in monkeys (Warwick, 1953). Using

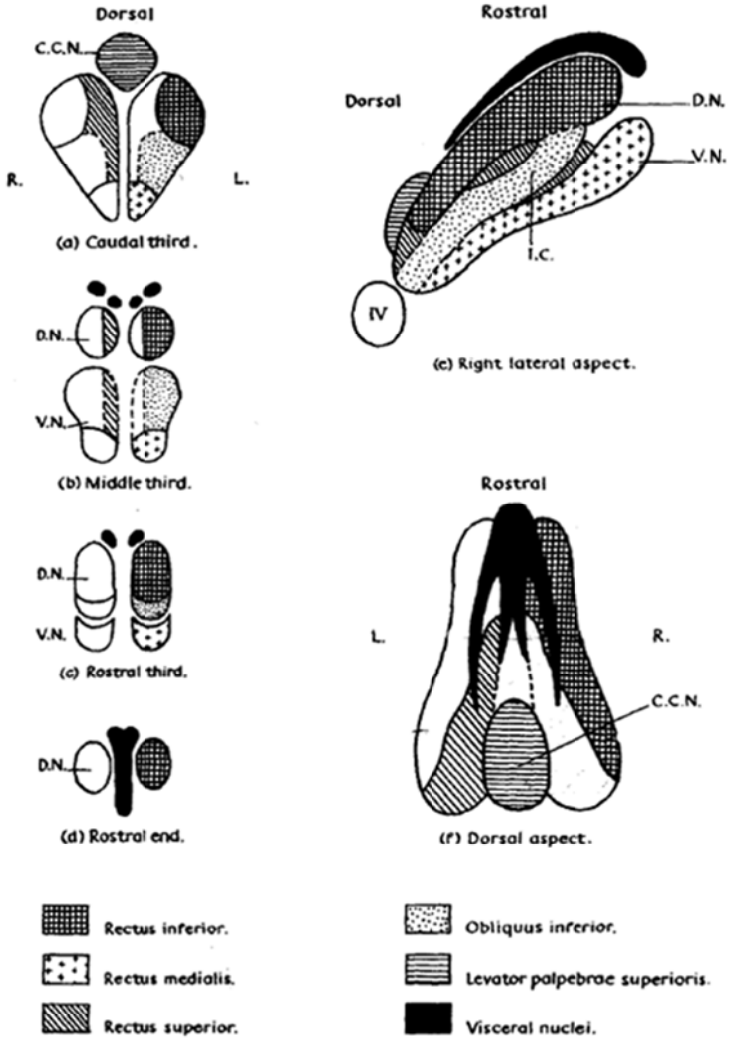

Fig. 21 Diagrams showing the representation of the right extra-ocular muscles in the oculomotor nucleus of the monkey. Transverse sections, at levels as indicated in the complex, are shown in (a)–(d). D.N. = dorsal nucleus, V.N. = ventral nucleus, C.C.N. = caudal central nucleus, I.C. = intermediate column, *IV* = trochlear nucleus.

Figure 3. Representation of motoneuronal groups in the oculomotor nucleus in monkey.
Schemes of the oculomotor nucleus in the transverse and horizontal plane showing the representation of the right extraocular muscles in monkey after extirpation of individual eye muscles (from: Warwick (1953) J. Comp. Neurol. 98:449-495).

the method of selective extirpation of single extraocular muscles and examining the areas with chromatolysis Warwick put forward a topographic map of the distribution of the subgroups of individual eye muscles within nIII of monkey. Accordingly, the IR subgroup is located rostro-dorsally, and the ventral MR subgroup appears throughout the whole length of nIII (Fig. 3).

1.2.4.2. Tract-Tracing Methods

Several methods of investigation resulted in conflicting opinions: stimulation, retrograde degeneration (chromatolysis analysis) methods, advanced techniques like the combination of immunhistochemical and tract tracing methods, were employed offering a broader platform for comparison of results. In one study horseradish peroxidase (HRP) was injected in the eye muscles innervated by the oculomotor nucleus (MR, IR, SR, IO) in eleven young adult baboons (Augustine et al., 1981). After 48 hours survival time, fixation and cutting, their brains were processed with tetramethylbenzidine (TMB)-HRP (Mesulam 1978) and analysed. According to Augustine (1981) the functional cell groups intermingled with each other in the nIII of baboon and could not be clearly identified as separate entities. Plotting of retrogradely labelled HRP-positive neurons following single injections of extrinsic eye muscles, the contralateral innervation of the superior rectus muscle was revealed. Motoneurons supplying the SR were located in the intermediate area of the contralateral nIII and the median raphe predominantly in the caudal two third of the nucleus. Retrogradely labelled IR motoneurons were found ipsilaterally, especially in the rostral third of the nIII. IO motoneurons where found ipsilaterally in the caudal two thirds of nIII occupying a similar portion as the SR of the contralateral eye but tend to lie more laterally. 57% of LP motoneurons were labelled on the ipsilateral side, while 43% were contralateral. Two subgroups of motoneurons were identified for the MR, which was confirmed in the Rhesus monkey by Büttner-Ennever and Akert, who called these MR populations A- and B-group (Fig. 4B; Büttner-Ennever and Akert, 1981). The A-group lies ventrally within nIII and reaches into the medial longitudinal fascicle (MLF), the B-group lie dorsolateral within nIII. A third small MR group, termed the C-group is located at the dorsomedial periphery of nIII (Büttner-Ennever and Akert, 1981). It contains motoneurons supplying the multiply-innervated non-twitch muscle fibres (MIFs) of the MR (Fig. 4C). Recent studies revealed that the C-group houses also the cell bodies of palisade endings, which are associated with MIFs at the myotendinous junction of the MR (Lienbacher et al., 2011). In addition, a group of motoneurons supplying the non-twitch muscle fibres of IO and SR are located between both nIII in the so-called S-group (Büttner-Ennever et al., 2001).

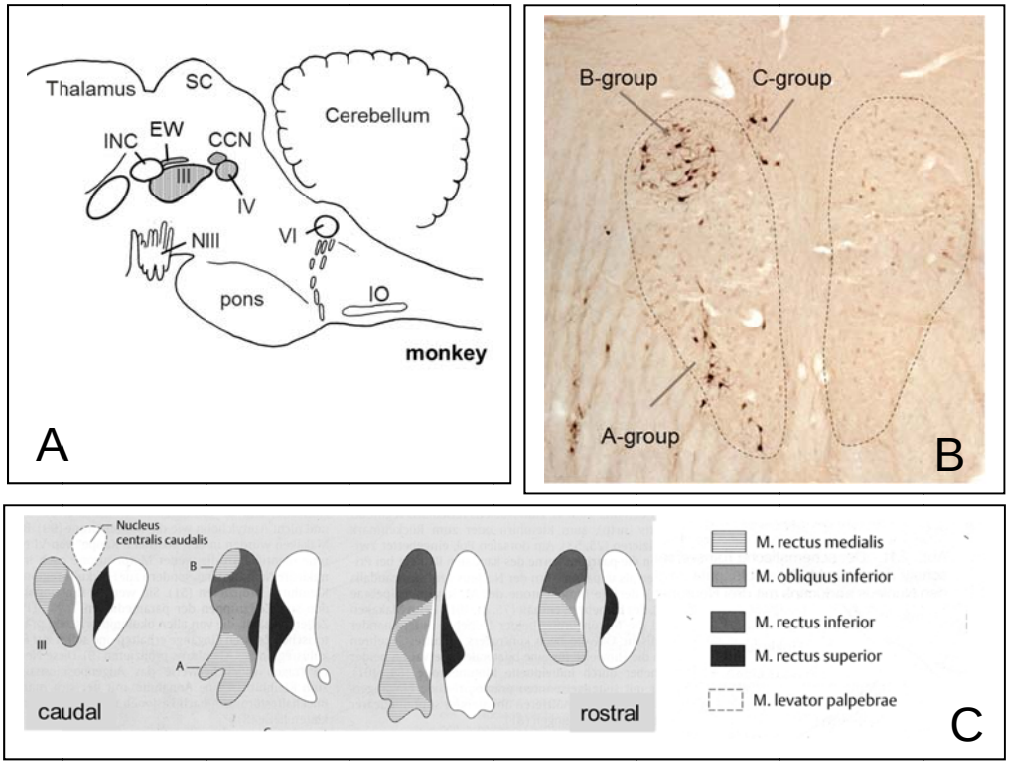

Figure 4. Representation of medial rectus motoneurons in the oculomotor nucleus
A: Schematic sagittal view of a monkey brainstem demonstrating the location of the oculomotor nucleus (III) including central caudal nucleus (CCN), the trochlear (IV) and abducens nucleus (VI). B: Detailed view of a transverse section through the oculomotor nucleus showing the location of labeled motoneurons in A-, B- and C-group after tracer injection into the left medial rectus muscle in monkey (MR). C: Scheme of transverse sections through III at different planes from caudal to rostral showing the location of motoneurons of individual eye muscles within boundaries of the oculomotor nucleus, and not those outside, like the C-group (see section 4.2.1). Figure 4c is part and modified version from "klinische Neuroophthalmologie" Hrs, Alfred Huber, Detlef Kömpf, Kapitel 2.2 S. 35, Abbildung 2.10.

1.3.3 Histochemistry of subgroups within III and IV

Immunostaining for the inhibitory transmitters glycine and GABA have shown in monkey that the motoneuronal subgroups subserving horizontal eye movements receive a strong supply of glycinergic terminals, whereas those for vertical eye movements receive a strong GABAergic input (Spencer et al., 1989; Spencer et al., 2003; Zeeh et al., 2015). Thereby in nIII the motoneuronal subgroups for MR are highlighted by their dense supply by glycinergic terminals and their relative lack from GABAergic terminals (Fig. 5A,B,E) (Spencer et al., 2003). Vice versa, the motoneurons of vertical moving eye muscles, i.e. SO, SR, IO, IR are highlighted by their dense GABAergic innervation. Moreover recent work from this laboratory has shown that in monkey the calcium-binding protein calretinin (CR) is primarily localized in nerve endings supplying the motoneurons subserving upgaze, i.e. SR and IO (Fig. 5E). In addition CR-positive terminals are abundant in the CCN (Fig. 5F), which contains the

motoneurons of the levator palpebrae muscle elevating the upper eyelid, which accompanies each upward eye movement (Zeeh et al., 2013). A strong glycinergic input to the CCN is present in addition (Horn and Büttner-Ennever, 2008).

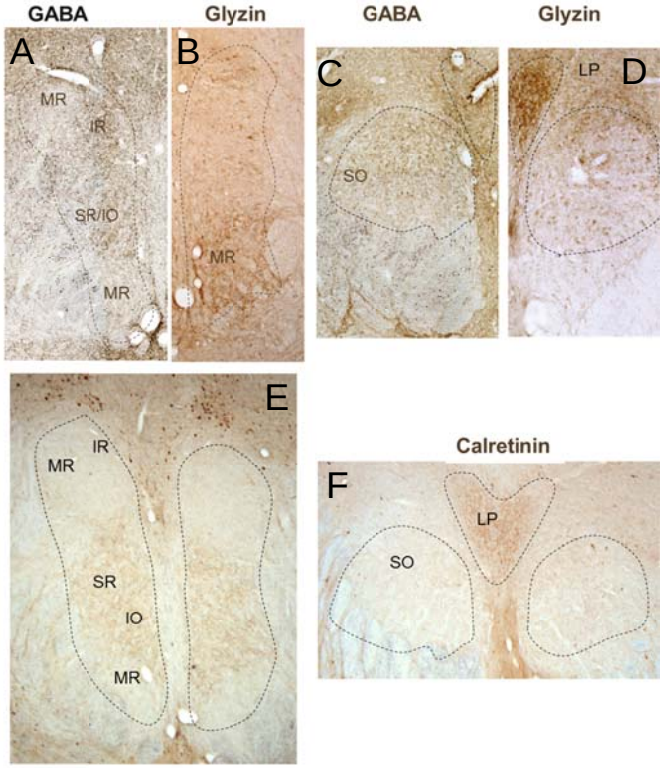

Figure 5. GABA and Calretinin inputs to motonuclei in monkey
Transverse sections through the oculomotor (A, B, E), central caudal and trochlear nucleus of monkey (C, D, F) immunostained for GABA (A, C), glycine (B, D) or calretinin (E, F). (Modified from Zeeh et al., 2013 Frontiers in Neuroanatomy 9:95, with permission from Zeeh et al.)

1.4. ANATOMICAL STUDIES OF OCULOMOTOR SUBGROUPS IN HUMAN

While the localization of functional subgroups of neurons in the perioculomotor region of humans has been analysed in previous studies (Edinger, 1885; Westphal, 1887; Perlia, 1889; Horn et al., 2008), the topographic representation and function of these nuclei of human, for example the Nucleus of Perlia (NP), are in many aspects unclear (Büttner-Ennever and Horn, 2014). Another example is the Edinger-Westphal nucleus (EW), which traditionally refers to the location of preganglionic neurons of the ciliary ganglion for pupillary constriction and lens accommodation. Since the discovery of the location of another cell group within this area, which contains the neuropeptide urocortin-1 (Vaughan et al., 1995), it has become obvious that the cytoarchitecturally defined “Edinger-Westphal nucleus” does not refer to the same cell group in different species. Cholinergic neurons correspond to the preganglionic parasympathetic neurons projecting peripherally via the oculomotor nerve to the ciliary

ganglion mediating pupillary constriction and lens accommodation (McDougal and Gamlin, 2011). In contrast the urocortin-1-expressing cell group is involved in circuits mediating food intake, alcohol consumption or stress (Gaszner et al., 2004; Giardino et al., 2011; Xu et al., 2012). With immunochytochemistry for cholinergic and urocortin markers the cytoarchitecturally defined EW in human was found to represent the urocortin-positive neurons and not the parasympathetic preganglionic cell group (Ryabinin et al., 2005; Horn et al., 2008; 2009). To facilitate better communication between researchers of different fields a new nomenclature has been introduced to distinguish between urocortin-positive centrally projecting neurons of the EWcp and cholinergic preganglionic neurons of the EW (EWpg), which are scattered dorsal to EWcp (Horn et al., 2008; Kozicz et al., 2011).

Unlike in monkey the organization of the neurons within the human nIII is less clear. There are several anatomical descriptions of the human nIII and nIV demonstrating subgroups based on cytoarchitecture mostly related to development (Pearson, 1944; Mann, 1927; Cooper, 1946; Yamaguchi and Honma, 2011; Yamaguchi, 2014) or cytoarchitecture of the nucleus (Le Gros Clark, 1926; Donzelli et al., 1998). Except for the unpaired central caudal nucleus (CCN), which innervates the levator palpebrae muscle (LP) (Schmidtke and Büttner-Ennever, 1992), it is still not clear, which subgroups innervate individual extraocular muscles in the human nIII, and different maps of the topographical arrangement of the motoneuron groups has been proposed for more than hundred years (Fig. 6) (Bernheimer, 1897; Brouwer, 1918), but in most textbooks on human anatomy a modified version of the map developed in monkey by Warwick (1953) is given (see Figure 3).

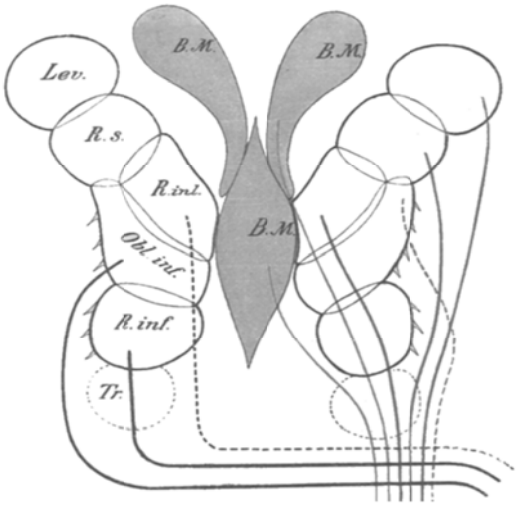

Figure 6. Early map of the human oculomotor nucleus
Schematic drawing of a horizontal section through the human brainstem to demonstrate the subgroups of the oculomotor nucleus. B.M.: Binnenmuskeln; Lev: levator palpebrae muscle; R.s. superior rectus muscle; R.int.: medial rectus muscle; Obl.inf.: inferior oblique muscle; R.inf.: inferior rectus muscle; Tr.: trochlear nucleus. (Figure 2 from Bernheimer, 1897, Arch. Ophthalmol 44: 481-525)

1.5. AIM OF THE PROJECT

Aim of this study is to investigate the location of the motoneuronal groups of individual extraocular eye muscles within the oculomotor nucleus in human by their differential histochemical profile based on previous studies in monkeys (Zeeh et al., 2013; 2015). The identification of the motoneuronal subgroups innervating individual extraocular muscles in human will help the clinical interpretation of disorders involving nIII lesions.

In this study frozen and paraffin sections from normal human post-mortem material was used. The cytoarchitecture of nIII and nIV was studied in classical Nissl and Gallyas fiber stainings and immunostaining for non-phosphorylated neurofilaments (NP-NF). Based on previous findings on the content on GABAergic and calretinin-positive terminals in different subgroups in monkey nIII, the histochemical features of the subgroups were investigated on parallel series of neighbouring sections with immunostaining for glutamate decarboxylase (GAD) and calretinin (CR) in the human material. In selected sections the motoneurons were in addition immunostained with ChAT-antibodies.

The results are part of a publication (Che Ngwa et al., 2014)

2 MATERIAL AND METHODS

2.1 MATERIALS

Four human brainstems were investigated in order to delineate the motoneuron subgroups within the oculomotor nucleus (nIII) and the trochlear nuclei (nIV) (Che Ngwa et al., 2014).

AUTOPSY REPORTS

Two brainstems from post-mortem human cases were obtained through the Reference Center for Neurodegenerative Disorders of the University of Munich (BrainNet) with written consent from next of kin, who confirmed the wishes at time of death. Two brainstems were obtained from donations to the Institute of Anatomy. All procedures were approved by the University ethic committees and obeyed the ethical standards laid down in the 1964 Declaration of Helsinki. It was of importance to acknowledge in the autopsy report that donors did not suffer from a neurological disease, which could have affected the brain stems and thus the outcome of the experimental results. All brainstems were obtained 24 hours after death. One brainstem was processed for frozen sections (case 1), while the other three cases were embedded in paraffin (case 2-4) (Table 2).

Case 1 (frozen sections): the donor was a 90 years old female, who had no neurological disease, but suffered from peripheral vascular disease 4^{th} grade. Death resulted from multi-organ failure. ***Case 2*** (paraffin sections): the donor was a 69 years old male without neurological disorders, but suffered in later life from Hodgkin disease, a side-effect due to several cycles of chemotherapy and Diabetes mellitus Type 2. Death resulted from metastasis in the cervical region of the spinal cord following squamous cell carcinoma in the temporal region. ***Case 3*** (paraffin sections): the donor was a 57 years old female without any mature macroscopic identification of neurological degeneration. She suffered from ovarian cancer, metastasis of lymph nodes und liver. Death occurred as a result of embolism of the lungs.

Case 4 (paraffin sections): the donor was a 67 years old male without neurological disorders. He suffered from rectal cancer. Death occurred as a result of left heart failure.

2.2. PREPARATION OF BRAINSTEMS

The cerebellum was removed by cutting through the cerebellar peduncles, and then the basilar arteries after the pontine branches were carefully dissected away. All brainstems were cut transversely through the superior colliculus and caudally about 3cm below the pyramidal

decussation. The brainstems of cases 1, 2 and 4 were further cut into two blocks as indicated in Figure 7, whereby the rostral block (A) contained the oculomotor (nIII) and trochlear nucleus (nIV). In addition, selected sections containing the oculomotor and trochlear nucleus were taken from case 3.

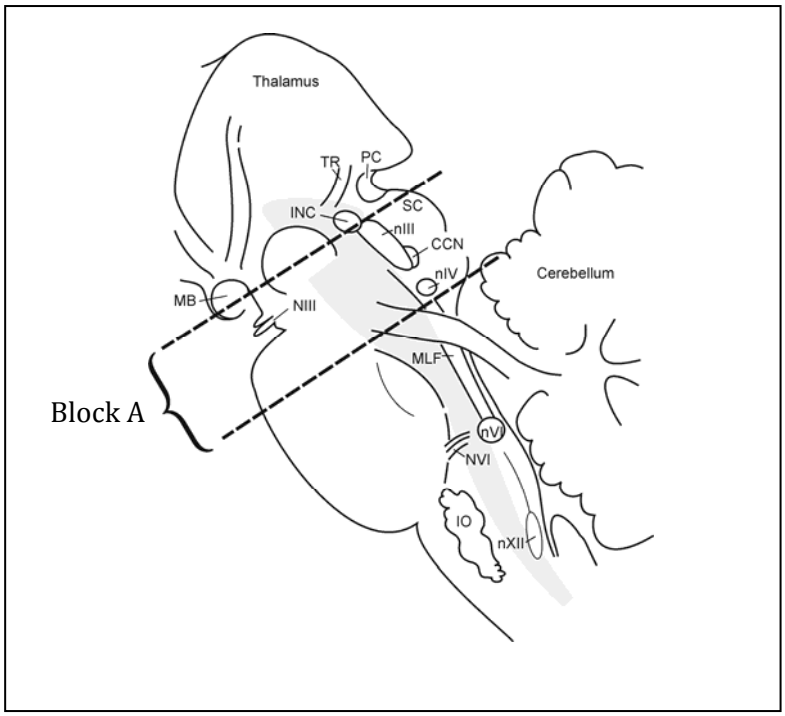

Figure 7. Blocking of the brainstem
Sagittal view of the human brainstem showing the block (dotted line) taken from the midbrain containing the oculomotor (nIII) and trochlear nuclei (nIV). CCN = central caudal nucleus; INC = interstitial nucleus of Cajal; IO = inferior olive; MB = mammillary body; MLF = medial longitudinal fascicle; NIII = oculomotor nerve; NVI = abducens nerve; nXII = hypoglossal nucleus; PC = posterior commissure; SC = superior colliculus; TR = tractus retroflexus.

2.3 FIXATION

To preserve the morphology of cells and the tissue antigens during subsequent processing, storage and immunohistochemical staining, an appropriate fixation was performed. However the effectiveness of fixation depends on fixation time, concentration of fixative and size of the brain stems. In the present study all tissue was immersed in either 4% paraformaldehyde in 0.1M phosphate buffer or 10% formalin at 4°C (Tab. 2). These fixatives prevent the tissues from autolysis through inactivation of endogenously released enzymes, decomposition of cells by bacteria or other microorganisms. In addition fixation hardens the tissue and aids sectioning (Romeis, 2010). For frozen sections the midbrain block of case 1 was transferred from fixative to 10% sucrose in PBS solution for 18 hours. After the brainstem had sunken to the bottom of the container in 10% sucrose solution, it was transferred to 20% sucrose in PBS

solution for 76 hours and finally in 30% sucrose solution for 48 hours. For paraffin embedding the midbrain blocks of case 2 and 4 were dehydrated in increasing concentrations of alcohol and xylene and then embedded in paraffin.

Case	Age	PMT	Fixative	TFT	Cutting	Thickness
1	90 years	24h	4% PFA	2 days	Frozen	40µm
2	69 years	24h	4% PFA	2 days	Paraffin	10 and 5µm
3	57 years	24h	10% FMN	6 days	Paraffin	10µm
4	67 years	24h	10% FMN	10 days	Paraffin	10 µm

Table 2: Human post-mortem cases used in the study
PMT= post mortem time, TFT= total fixation time, FMN= Formalin, PFA= Paraformaldehyde

2.4 SECTIONING

For freeze cutting (case 1) the brainstem block was wrapped up in aluminium foil and embedded in dry ice for 10 minutes. Then the frozen block was placed on the specimen holder of the cryostat using a mounting medium (Tissue Tec). Serial sections at 40µm were collected from caudal to rostral. Every 7th section was immediately mounted on a slide for Nissl staining (interval of 240µm), the respective neighbouring sections for Gallyas staining. Additional 4 series were collected in cold PB for free-floating immunostaining with antibodies against either non-phosporylated neurofilaments (NF-NF) or glutamic acid decarboxylase (GAD).

Case 2 and 4: From paraffin blocks series of 20 consecutive sections of 10µm and 10 consecutive sections of 5µm were cut alternately from rostral to the caudal end of the brain stem and mounted on superfrost slides. Every 40^{th} section of 10µm thickness (1, 40, 80 etc) was stained with cresyl violet. The neighbouring sections were stored at room temperature to be processed immunoperoxidase labelling of different markers, e.g. choline acetyltransferase (ChAT) and either GAD or calretinin (CR).

Case 3: Selected paraffin sections of a case that had been cut at 10µm sections were processed for the immunohistochemical detection of ChAT and GAD.

2.5. STAINING TECHNIQUES

2.5.1 NISSL STAINING

The classical Nissl-staining method labels neurons and glial cells and is used to demonstrate the cytoarchitecture of brain tissue. It was named after Franz Nissl, a German neuropathologist who developed the technique in the Anatomy Department at the Ludwig Maximilians University. It stains the rRNA in the ribosomes on the rough endoplasmic reticulum of neurones (Nissl Substance) in a purple/dark blue colour (Romeis, 2010). Here cresyl violet is used to identify nIII and nIV within the midbrain tegmentum (detailed protocol see appendix).

2.5.2 GALLYAS STAIN

The Gallays method was used to visualize the myelin of nerve fibers in the midbrain. It is a silver staining using a physical developing procedure described by Gallyas (Gallyas, 1979). (For detailed procedures see protocol).

2.5.3 IMMUNOHISTOCHEMICAL STAINING

For the delineation of the motoneuronal subgroups in the human nIV and nIII, several series of neighbouring sections were treated with antibodies against different antigens, e.g. non-phosphorylated neurofilaments (NP-NF), choline acetyltransferase (ChAT), glutamate decarboxylase (GAD) and calretinin (CR) with immunoperoxidase detection. A summary of the antibody sources and detection methods is given in Table 3.

NON-PHOSPHORYLATED NEUROFILAMENT (NP-NF)

The monoclonal mouse antibody (SMI-32, Sternberger) reacts with non-phosphorylated epitope in neurofilament H and is abolished when the epitope is phosphorylated (Sternberger and Sternberger, 1982). This antibody visualizes two bands (200 and 180kDa) in conventional immunoblots (Goldstein et. al, 2003). The non-phosphorylated neurofilament stain (NP-NF) has been proven to label the motoneurons in their whole extent including the dendrites and the axons (Eberhorn et al. 2005). It was used here to demonstrate the respective motoneuron subgroups in nIII and nIV in one case (case 1).

CHOLINE ACETYLTRANSFERASE (CHAT)

Detailed characterization and distribution of cholinergic motoneurons in nIII and nIV were studied by staining with a polyclonal antibody against the synthetizing enzyme choline acetyltransferase (ChAT) raised in goat (AB 144P; Chemicon). The antigen was purified from

human placenta. It is identical to the brain enzyme (Bruce et al., 1985) (see protocol for details)

GLUTAMATE DECARBOXYLASE (GAD)

GABAergic terminals were detected by using a mouse monoclonal antibody directed against both isoforms of the GABA synthesizing enzyme glutamate decarboxylase (GAD) (Biotrend: GC3108). In mammals, GAD exists in two isoforms GAD_{67} and GAD_{65} encoded by different genes. Both forms are expressed in the brain, where GABA is used as the transmitter. GAD_{65} is an amphiphilic, membrane-anchored protein (585aa), encoded on human chromosome 10, and is responsible for vesicular GABA production. GAD_{67} is cytoplasmic (594aa.), encoded on chromosome 2, and seems to be responsible for significant cytoplasmic GABA production. GAD expression changes during neural development in rat spinal cord. GAD_{65} is expressed transiently in commissural axons around E13 but is down regulated the next day while GAD_{67} expression increases mostly in the somata of those neurons (Phelps et al. 1999).

CALRETININ (CR)

A rabbit polyclonal antibody (7699/4, LOT 18299, Swant, Bellinzona, Switzerland) against calretinin (CR) was used. CR is a calcium-binding protein of the EF-hand family related to calbindin D-28k and calmodulin with a widespread distribution throughout the brain (review: Andressen et al. 1993). The CR antiserum was produced in rabbits by immunization with recombinant human CR containing a 6-his tag at the N-terminal C.

2.5.3.1 Single immunostaining for NP-NF, GAD, CR

Parallel series of adjacent frozen sections were processed free-floating, whereas the paraffin sections were processed on slide after deparaffination in three changes of xylene and rehydration in decreasing concentrations of alcohol (100%, 96%, 90%, 70%) and a final rinse in distilled water. In addition, the paraffin sections of formalin-fixed tissue underwent an antigen retrieval procedure preceding the protocol for immunostaining: after deparaffination the sections were incubated in 0.01M sodium citrate buffer (pH 8.5) in a water bath at 80°C for 15 min and then for another 15 min at room temperature, before being rinsed and started with the immunostaining protocol (Jiao et al., 1999). An overview of the sources and dilutions of antibodies is given in Table 2.

After a short rinse in distilled water and 0.1M PBS, pH 7.4, the sections were treated with 1% H_2O_2 for 30 minutes to eliminate endogenous peroxidase activity and washed extensively with 0.1M TBS (pH 7.4). To block non-specific bindings sites the sections were then preincubated with 2% normal horse serum in 0.3% Triton-X 100 in 0.1M TBS for 1 h at room temperature. Parallel 2mm spaced series of neighboring sections were subsequently treated either with mouse anti-NP-NF (1:6000; Sternberger) or mouse anti-GAD (1:4000; Biotrend) or rabbit anti-CR (1:2500; SWant) for 2 days at room temperature. After washing in 0.1M TBS, the sections were incubated either in biotinylated horse anti-mouse IgG (1:200; Vector Laboratories) or biotinylated horse anti-rabbit IgG (1:200; Vector Laboratories) at room temperature for 1 h, followed by 3 washes in 0.1M TBS. Then sections were incubated in extravidin-peroxidase (EAP; 1:1000; Sigma) for 1h at room temperature. The glycoprotein avidin has a high affinity to biotin and therefore binds to the biotinylated secondary antibodies. After two rinses in 0.1M TBS and one rinse in 0.05M Tris-buffer (TB), pH 8, the peroxidase of the EAP complex indicating the antigenic sites was visualized by a reaction in 0.025% diaminobenzidine and 0.015% H_20_2 in 0.05M TB for 10 min. After several rinses in TBS free floating sections were mounted, air-dried, dehydrated in increasing concentrations of alcohol, then immersed in xylene and coverslipped in Depex (Serva, Heidelberg, Germany).

2.5.3.2 Combined immunoperoxidase labeling for ChAT and GAD

In selected paraffin sections combined immunoperoxidase labeling was used to simultaneously detect ChAT and GAD. After deparaffination and rehydration, the sections were washed in 0.1M Tris-buffered saline (TBS, pH 7.4), treated with 1% H_2O_2 in TBS for 30 min, were rinsed again, and preincubated with 2% normal rabbit serum in 0.3% Triton-X 100 in TBS for 1 h at room temperature. The sections were then treated with goat anti-ChAT (1:100; Chemicon, AB144P) in TBS with 2% rabbit serum and 0.3% Triton X-100 for 48h at room temperature. After three washes in 0.1M TBS the sections were incubated in biotinylated rabbit anti-goat IgG (1:200, Vector lab) in TBS containing 2% bovine serum albumin for 1h at room temperature. After three washes in 0.1M TBS the sections were treated with extravidin-peroxidase (EAP; 1:1000; Sigma) for 1h. Then, two rinses with 0.1M TBS were followed by one wash with 0.05M Tris-buffer, pH 8, and the reaction with 0,025% diaminobenzidine, 0.4% ammonium nickel sulfate and 0,015% H_20_2 in 0.05M Tris-buffer, pH 8, for 10 min. This results in a black staining of ChAT-positive structures. After a thorough washing and blocking of residual peroxidase activity with 1% H_20_2 in 0.1M TBS, the sections

were preincubated in 2% normal horse serum in 0,3% Triton-X-100 in 0.1M TBS for 1 h at room temperature before transferred to mouse anti-GAD (1:4000; Biotrend) in 2% normal horse serum and 0.3% Triton-X-100 in TBS for 48h at room temperature. After three rinses in 0.1M TBS the sections were incubated in biotinylated horse anti-mouse IgG (1:200; Vector laboratories, Burlingame, CA, USA) in TBS containing 2% bovine serum albumin for 1 h at room temperature. The antigen binding sites were detected by incubating sections in extravidin peroxidase (1:1000; Sigma, St. Louis, MO, USA) for 1 h and a subsequent reaction with 0.025 % diaminobenzidine and 0.015% H_2O_2 in 0.05 M Tris-buffer (pH 7.6) for 10 min to yield a brown staining of GAD-positive profiles. After washing, the sections were air-dried, dehydrated in alcohol and coverslipped with DPX (Sigma, St. Louis, MO, USA).

Antigen	Primary Antibody	Manufactor	Secondary antibody
Non-phosphorylated neurofilamet (NP-NF)	Mouse anti-NP-NF 1:5000	Sternberger Monoclonals incorporated: Cat-No: SMI 32	Biot. Horse anti-mouse 1:200 (Vect. Lab.)
Glutamate decarboxylase (GAD)	Mouse anti GAD, 1:4000	Biotrend, GC3108	Biot. Horse anti-mouse 1:200 (Vect. Lab.)
Choline acetyltransferase (ChAT)	Goat anti-ChAT, 1:100	Chemicon, AB144P	Biot. Rabbit anti-goat, 1:200 (Vect. Lab.)
Calretinin (CR)	Rabbit anti-Calretinin 1:2500	SWant, 7699/4	Biot. Horse anti-Rabbit 1:200 (Vect. Lab.)

Table 3: Sources and dilution of primary antibodies

2.6. DIGITAL IMAGE ANALYSIS

All slides were examined with a light microscope DMRB (Bensheim, Germany; or Zeiss Axiophot). Brightfield photographs were taken with a digital camera (Microfire; Optronics, USA) mounted on the microscope (Zeiss, Axiophot). The images were captured on a computer with Picture frame software 2.2. (Optronics, USA) and processed in Photoshop 7.0 (Adobe Systems, Mountain View, CA). The sharpness, contrast, and brightness were adjusted to reflect the appearance of the picture seen through the microscope. Arrangement and labelling of pictures was performed with drawing software (CorelDraw 11) or in Powerpoint (Microsoft, 2010).

2.7. SEMIQUANTITATIVE ESTIMATION OF GAD- AND CR-POSITIVE TERMINAL DENSITY

A semiquantitative approach was chosen for a judgment of the density of GAD- and CR-positive input to motoneurons in nIII and nIV. For that all subgroups in nIII and nIV were viewed at high-power magnification and the density of GAD- and CR-positive puncta was judged as either very strong, moderate to strong, or weak and accordingly marked in a series of schematic views of nIII and nIV. Were present, immunoreactive cell bodies were included in the scheme in a non-quantitative manner (Fig. 16). In a subsequent study with additional markers for glycinergic inputs a systematic quantitative analysis with statistics was performed in parallel to a similar investigation in rhesus monkey (Che Ngwa et al., 2014; Zeeh et al., 2015).

3 RESULTS

The general cytoarchitecture of the human trochlear (nIV) and oculomotor nucleus (nIII) was studied in Nissl- and Gallyas-staining and immunohistochemistry for non-phosphorylated filaments (NP-NF). A delineation and mapping of the individual subgroups of motoneurons within nIII was achieved with simultaneous immunostaining for ChAT and GAD or for CR. A semiquantitative judgment of the density of GABAergic and CR input served as basis for the delineation of subgroups within nIII. A preliminary quantitative estimation of the GABAergic input served as basis for a more elaborated quantitative analysis of GAD-positive and CR-positive inputs, which were combined with the analysis of glycin-positive inputs carried out by colleagues of the research group and published in a common paper (Che Ngwa et al., 2014).

3.1. TROCHLEAR NUCLEI

3.1.1. CYTOARCHITECTURE

Coming from the caudal direction the trochlear nucleus (nIV) is clearly outlined in Nissl and Gallyas staining as a round nucleus embedded in the fibers of the medial longitudinal fascicle (MLF) (Fig. 8A, B). As reported by others two completely separated divisions of the nIV are apparent in the caudo-rostral direction (Büttner-Ennever and Horn, 2014). In NP-NF-immunostained sections, the morphology of the motoneurons in nIV was also well delineated (Fig. 8C). The dendrites remained confined to the dorsal boundaries of the nucleus. Most axons leave the nucleus laterally to form the trochlear nerve, which exits the brainstem at its dorsal side. However some axons were also observed travelling between the bundles of the MLF leaving ventrally (Fig. 8C, arrows).

3.1.2. HISTOCHEMICAL PROPERTIES OF nIV

All neurons within nIV were immunostained for ChAT. Double-immunostained sections revealed that ChAT-positive motoneurons receive a strong input from GAD-positive terminals (Fig. 8F). Immunostaining for calretinin (CR) revealed that no CR-positive neurons were present in nIV, and only few scattered CR-positive puncta were found within the neuropil of nIV (Fig. 8G).

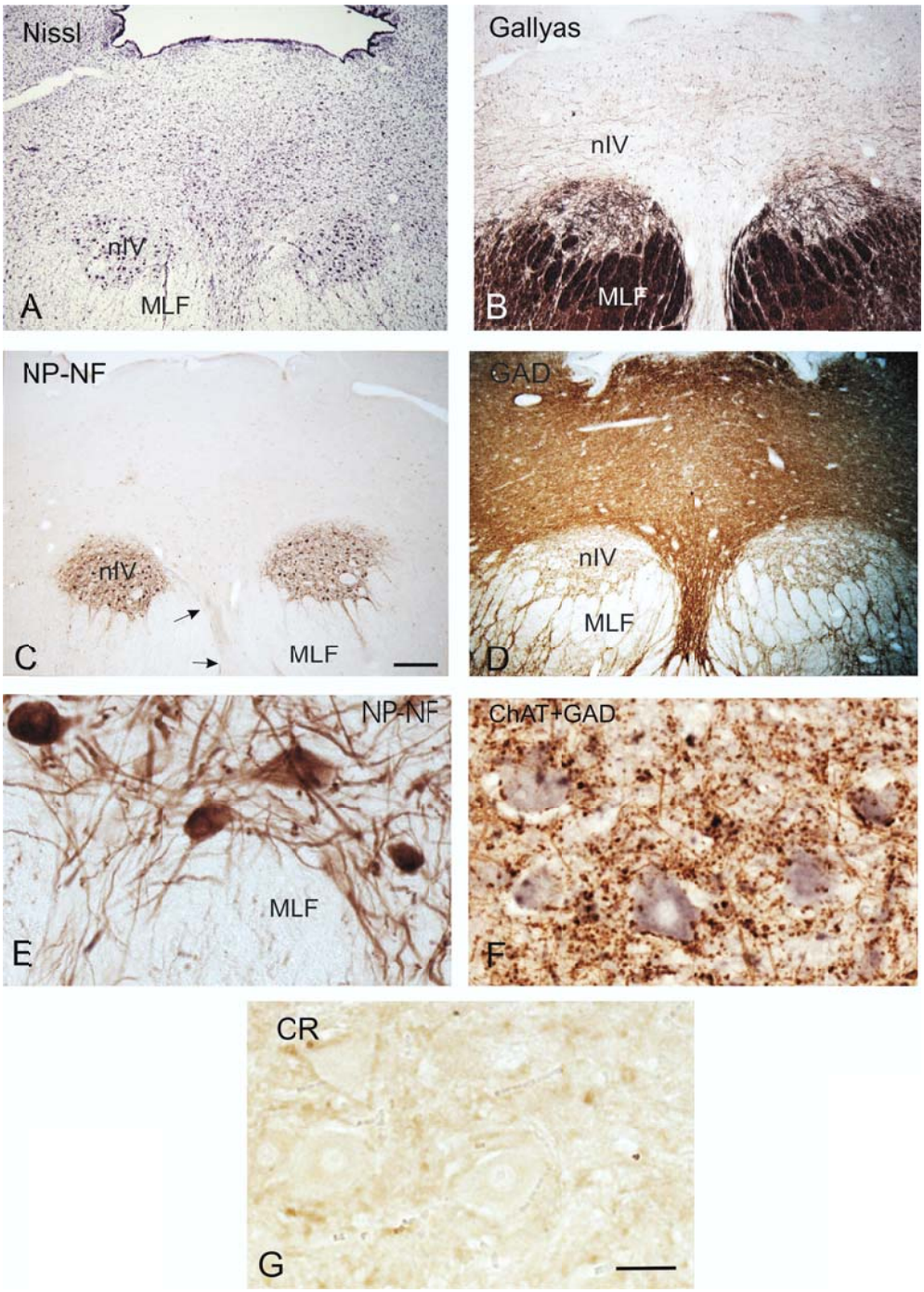

Figure 8. Transverse sections through the human trochlear nucleus.
Neighbouring transverse sections through the human brainstem at the plane of the trochlear nucleus (nIV) stained for Nissl (A), Gallyas fiber stain (B), non-phosphorylated neurofilaments (NP-NF) (C, E) to reveal the cytoarchitecture, and immunostaining for GAD (D, F) and calretinin (CR) (G). Note the fibers leaving the trochlear nucleus and travelling ventrally medial to the fibres of the medial longitudinal fascicle (C arrows, E). A high number of GAD-positive puncta (F, brown) is associated with cholinergic (black) motoneurons, whereas no CR-positive profiles are found within nIV (G). Scale bar in C: 500µm (applies to A, B, D); in G: 30µm (applies to E, F). "A modified version of this figure is published in Che Ngwa et al., 2014, Frontiers in Neuroanatomy 8:2"

3.2. OCULOMOTOR NUCLEUS

3.2.1 CYTOARCHITECTURE

At its caudal end the nIII appears as a V-shaped nucleus with the unpaired central caudal nucleus (CCN) containing the levator palpebrae (LP) motoneurons (Fig. 9A, B. C). In NP-NF-immunostaining a lateral group (LAT) of scattered neurons within the MLF is most apparent, which appears separated from a compact central cell group (CEN) (Fig. 9C). A small dorsomedial group (DM) can be delineated from a small dorsolateral cell group (DL), which forms an almost circle-like round cluster at this plane of nIII (Fig.9 A, C). In Gallyas staining it is apparent that a bundle of fibers leaves the dorsolateral subgroup (DL) and runs between DM and CEN subgroups (Fig. 9B). An even clearer cytoarchitectural picture of the motoneurons was revealed in the NP-NF stain. The dendrites of the motoneurons are intermingled with each other most apparent for the CEN subgroup. At further rostral levels, the nIII elongates dorso-ventrally and approaches the midline from both sides with the rostral end of the CCN situated dorsally (Fig. 10A). At this level five separate groups can be delineated within the nIII with NP-NF staining (Fig. 10C): these are the CEN, DM, LAT and DL and an additional ventral group (VEN). In Gallyas staining it is apparent that these groups are separated by traversing fibers, whereby the DL is most pronounced, almost encapsulated by fibers (Fig. 10 B, C).

At the plane where the rostral end of the CCN is disappearing, a small group of densely packed neurons adjacent to the dorsal rim of nIII becomes apparent in Nissl-stained sections (Fig. 10A). It is known now to be part of the perioculomotor urocortin group forming a central projecting part of the Edinger-Westphal nucleus (EWcp) (Horn et al. 2008; Kozicz et al. 2011). At further rostral planes the medial portion of the EWcp appears sandwiched between the dorsal parts of nIII of both sides (Fig. 11A). At about the same level at the midline ventrally, a cell group known as the Nucleus of Perlia (NP) is separated by dorso-ventrally traversing fibers from the main nucleus (Perlia 1889) (Fig. 11 A, B, C). As described previously the NP shows a similar pattern of NP-NF immunoreactivity as the motoneurons in nIII (Fig. 11C). The NP extends up to the rostral end of nIII (Fig. 12). At the most rostral level the main nIII nuclei, consisting of the DL group, are embraced by the EWcp forming a large cell group dorsally and a small extension ventrally (Fig. 13A), which does not express NP-NF immunoreactivity (Fig. 13C). With NP-NF-immunostaining scattered neurons are visible dorsal to EWcp, which may correspond to the parasympathetic preganglionic neurons of the

EW (EWpg) projecting to the ciliary ganglion (Fig. 13C) (Horn et al., 2008; Kozicz et al., 2011).

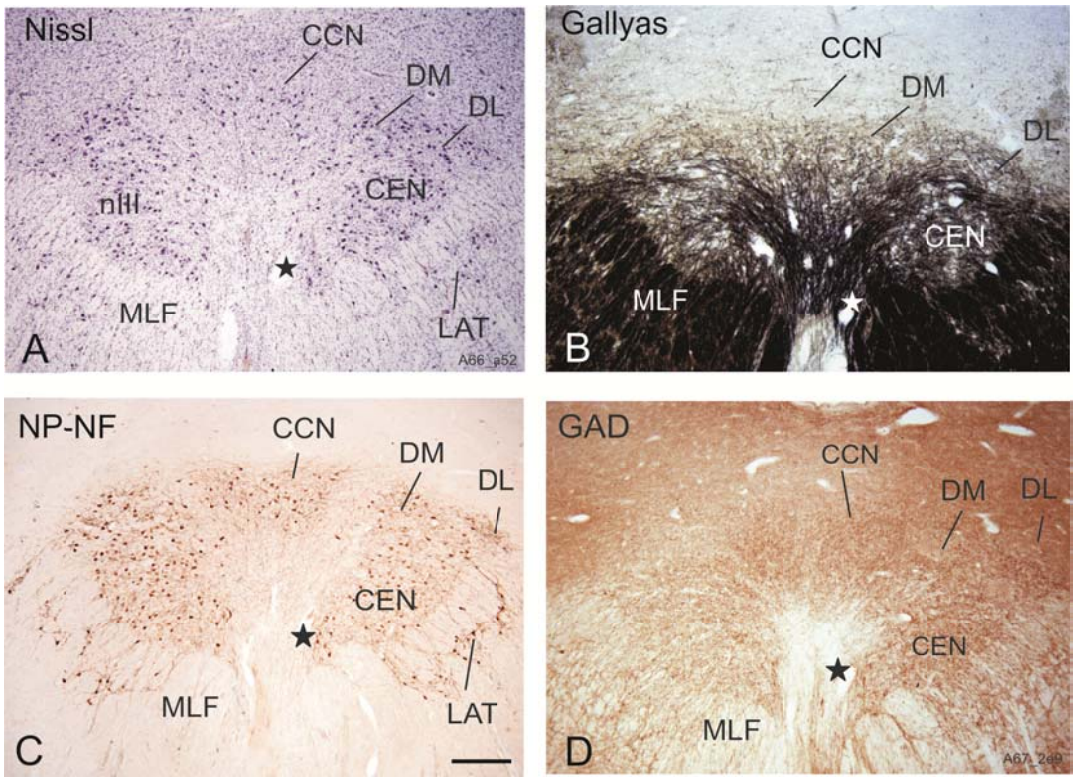

Figure 9. Transverse sections through the central caudal nucleus
Neighbouring transverse sections through the human brainstem at the plane of the central caudal nucleus (CCN) stained for Nissl (A), Gallyas fiber stain (B), non-phosphorylated neurofilaments (NP-NF) (C) to reveal the cytoarchitecture and GAD-immunostaining (D). For clarity a star labels the same blood vessel in neighbouring sections. Note that a lateral group (LAT) is separated from the main oculomotor nucleus by the fibers of the medial longitudinal fascicle (MLF). DL= dorsolateral subgroup, DM= dorsomedial subgroup, CEN= central subgroup, VEN= ventral subgroup, LAT= lateral subgroup. Scale bar in C = 500µm (applies to A, B, D). "A modified version of this figure is published in Che Ngwa et al., 2014, Frontiers in Neuroanatomy 8:2"

3.2.2. Histochemical Properties of Oculomotor Subgroups.

3.2.2.1 Central caudal nucleus

The CCN could be detected only in cross sections of the caudal nIII as a separated unpaired nucleus dorsal to nIII (Fig. 9, 10). The NP-NF staining demonstrated that the CCN is clearly separated from the main nIII (Fig. 9C, 10C) by traversing fibers from the DM and DL groups apparent from Gallayas staining (Fig. 9B, 10B). Especially on caudal planes the CCN was highlighted by its strong supply from GAD-positive puncta (Fig. 9D), which were distributed along the outlines of the cell bodies and dendrites of the ChAT-positive motoneurons and in

the neuropil (Fig. 14G). In addition, CCN receives a strong supply from CR-positive fibers and puncta (Fig. 10E, 15 G).

3.2.2.2 Dorsolateral subgroup (DL)

The dorsolateral subgroup (DL) receives a rich supply of GAD-positive terminals, which outlines its boundaries, already apparent in an overview (Fig. 9D). At high magnification it is apparent that the GAD-positive puncta are associated with the somata and dendrites of the ChAT positive motoneurons (Fig. 14A). As nIV the DL contains only very few CR-immunoreactive neuronal profiles most of them traversing fibers (Fig. 15. A). At the rostral end of nIII the NP-NF staining revealed that fibers of neurons within the DL cross over the midline to its contralateral counterpart (Fig. 13 C, arrow; E)

3.2.2.3 Dorsomedial subgroup (DM)

The dorsomedial subgroup (DM) could also be identified in the Nissl stain and showed its largest cross section area at mid-level sections of nIII (Fig. 11A). It is bordered from traversing fibers at its lateral and medial borders – apparent in Gallyas staining (Fig. 11B). In addition, the DM subgroup has a supply of GABAergic inputs, which is markedly less than the DL, NP and EWcp. This property was taken to judge whether at the most rostral level of nIII the DL or DM was present (Fig. 13 A, B, C, D). CR-immunostaining did not reveal any labeled cells or puncta and fibers within DM (Fig. 15 C).

3.2.2.4 Ventral subgroup (VEN)

The ventral subgroup (VEN) could be identified in the Nissl stain forming a separated group extending throughout almost the complete length of nIII (Fig. 10, 11, 12). Gallyas staining revealed its delineation from the medial Nucleus of Perlia (NP) by vertically traversing fibers at the medial border of VEN (Fig. 10B, 11B, 12B). No clear separation from the neighbouring subgroups was seen with immunostaining for NP-NF (Fig. 10C, 11C, 12C).
The VEN subgroup received a strong supply of GABAergic terminals similar to that of the DL subgroup (Fig. 10D). The detailed view shows numerous GAD-positive puncta attached to the outlines of ChAT-positive motoneurons (Fig. 14D). As noted for most other subgroups no CR-positive neuronal elements were found in VEN in contrast to the adjacent CEN (10E, 11E).

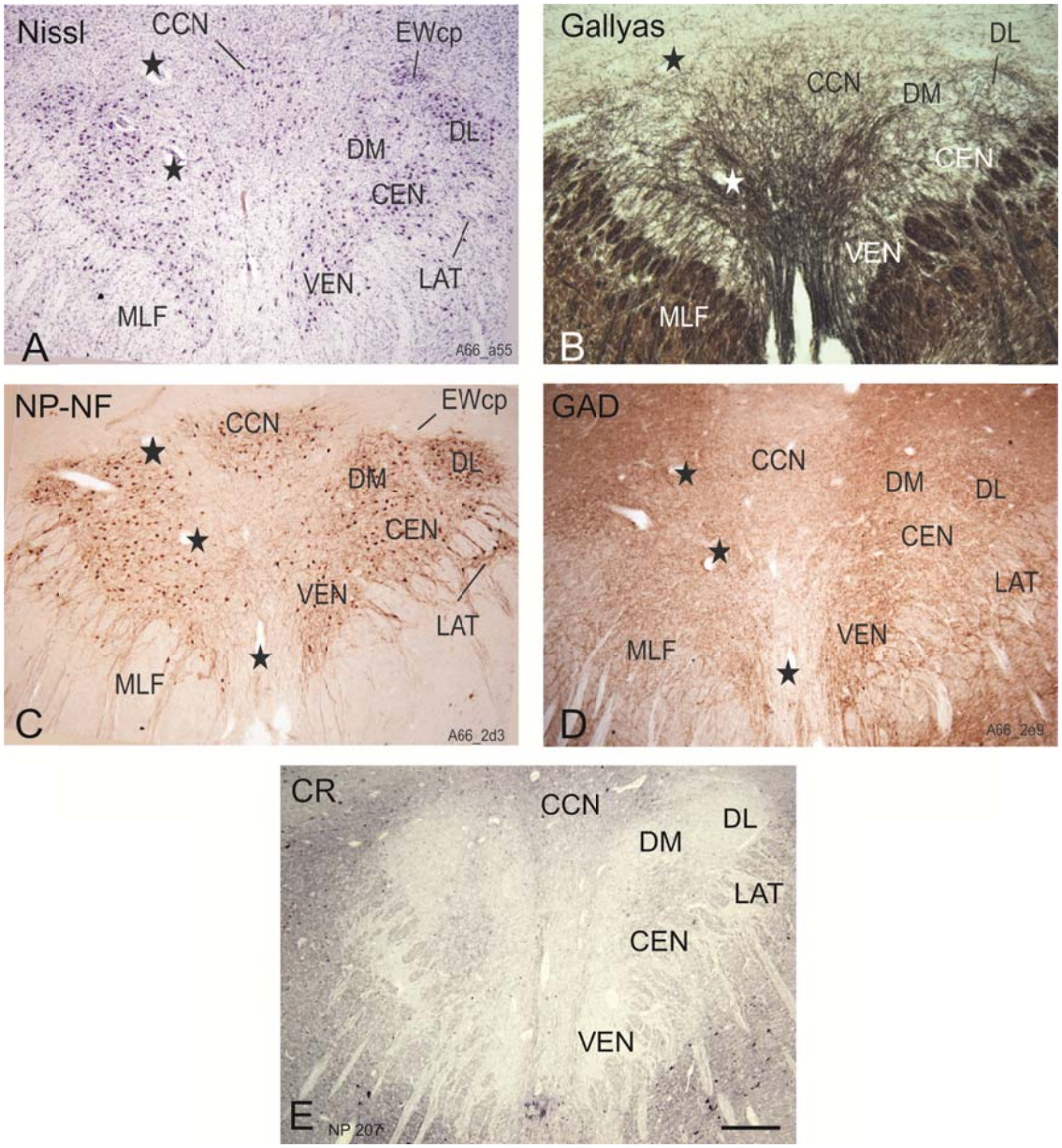

Figure 10. Transverse sections through the caudal oculomotor nucleus

Neighbouring transverse sections through the human brainstem at the plane of the caudal half of the oculomotor nucleus through the rostral central caudal nucleus (CCN) stained for Nissl (A), Gallyas fiber stain (B), non-phosphorylated neurofilaments (NP-NF) to reveal the cytoarchitecture (C) and GAD-immunostaining (D). Three blood vessels (Stars) serve as landmarks. Note that the dorsolateral (DL) and ventral subgroup (VEN) are most densely labelled in GAD-staining (D), whereas the CCN and central group (CEN) receive a strong supply from CR-positive profiles (E). DM= dorsomedial subgroup, VEN= ventral subgroup, LAT= lateral subgroup, MLF = medial longitudinal fascicle. Scale bar A-E: 500µm. "A modified version of this figure is published in Che Ngwa et al., 2014, Frontiers in Neuroanatomy 8:2"

3.2.2.5 Lateral subgroup (LAT)

The lateral subgroup (LAT) is only visible at caudal transverse sections of nIII (Fig. 10A, C, D) and may belong to adjacent subgroups within nIII, but being separated by the traversing fibers of the MLF as found in monkey for the MR subgroups (Büttner-Ennever et al., 1981). From NP-NF stains it is apparent that the dendrites of the motoneurons reach into the CEN and VEN of nIII (Fig. 9C, 10C). A strong supply from GABAergic terminals was found on somata and dendrites of ChAT-positive neurons (Fig. 14E). As in VEN, the LAT cell group does not show an expression of CR-positive punctate profiles, but a few traversing CR-fibers are visible, which may enter from the MLF (Fig. 15E).

3.2.2.6. Central subgroup (CEN)

On caudal sections the central group lies at the ventrolateral border of nIII as a large cell group located between the DL dorsally and VEN ventrally (Fig. 9, 10, 11). It extends through the caudal half of nIII. It is separated from the dorsal adjoining DM and DL by the dorsoventrally running fibers seen in the Gallyas stain (Fig.9B, 10B, 11B). The delineation of CEN is not so obvious from NP-NF stains, since the dendrites extend into neighbouring subgroups except the DL (Fig. 9C, 10C, 11C). As DL the CEN subgroup receives a strong supply of GABAergic terminals covering the somata and dendrites of ChAT-positive motoneurons (Fig. 9D, 10D, 11D, 12D, 14B). A significant observation for CEN was the presence of numerous CR-positive fibers and puncta highlighting this group within nIII very clearly (Fig. 10E, 11E). The close inspection revealed that the motoneurons in CEN were associated with many CR-positive puncta and fibers entering the nIII from the adjacent lateral MLF (Fig. 15 B).

3.2.2.7 Nucleus of Perlia (NP)

The nucleus of Perlia (NP) could be identified in the Nissl stain as cytoarchitectural entity throughout the rostral half of nIII (Fig. 11, 12). It is located at the midline as an unpaired nucleus and separated at its lateral boundaries from the nIII by longitudinally running fibers clearly visible with Gallyas staining (Fig.11B, 12B). These fibers expressed strong CR-immunostaining (Fig. 11E, 12E). The neurons of NP showed a strong NP-NF immunoreactivity as described earlier (Horn et al., 2008) (Fig. 11C, 12C). The neurons within NP received a moderate supply by GABAergic puncta (Fig. 14F) and it was filled with numerous CR-positive fibers and puncta associated with the neurons (Fig. 15 F).

3.2.2.8 Urocortin-positive centrally projecting neurons of EW

In this study the centrally projecting neurons of EW (EWcp) have not been outlined with urocortin-immunostaining, since this has been demonstrated clearly in previous reports (Ryabinin et al., 2005; Horn et al., 2008). From these studies it is clear that the urocortin-containing EWcp is clearly visible and defined in Nissl-stainings as a compact chromatophilic group of small-elongated cell bodies dorsal to DM (Fig. 10A, 11A) and DL (Fig. 12A, 13A). At rostral levels the dorsally located EWcp enlarges and a second smaller ventral group of EWcp is visible (Fig. 13A). Rostral to nIII this cell population merges with the anteromedian nucleus, which may represent a rostral extension of EWcp. This reflects the topographical arrangement of EWcp and nIII (see Büttner-Ennever and Horn, 2014). As described earlier the neurons of EWcp are not ChAT- or NP-NF-positive (Fig. 10C, 11C, 12C, which was taken as indication that they do not represent parasympathic preganglionic neurons of the ciliary ganglion in an earlier study (Horn et al., 2008). The non-cholinergic neurons of EWcp received the strongest supply of GABAergic terminals found in this study (Fig. 14H). This was the only subgroup, where scattered CR-positive neurons were found (Fig. 11E, 12E, 15H; 16F, 16H, 16K, 16M). They may represent the source of the CR fibers traversing dorsoventrally separating the NP from the main nIII on both sides (Fig. 11E, 12E).

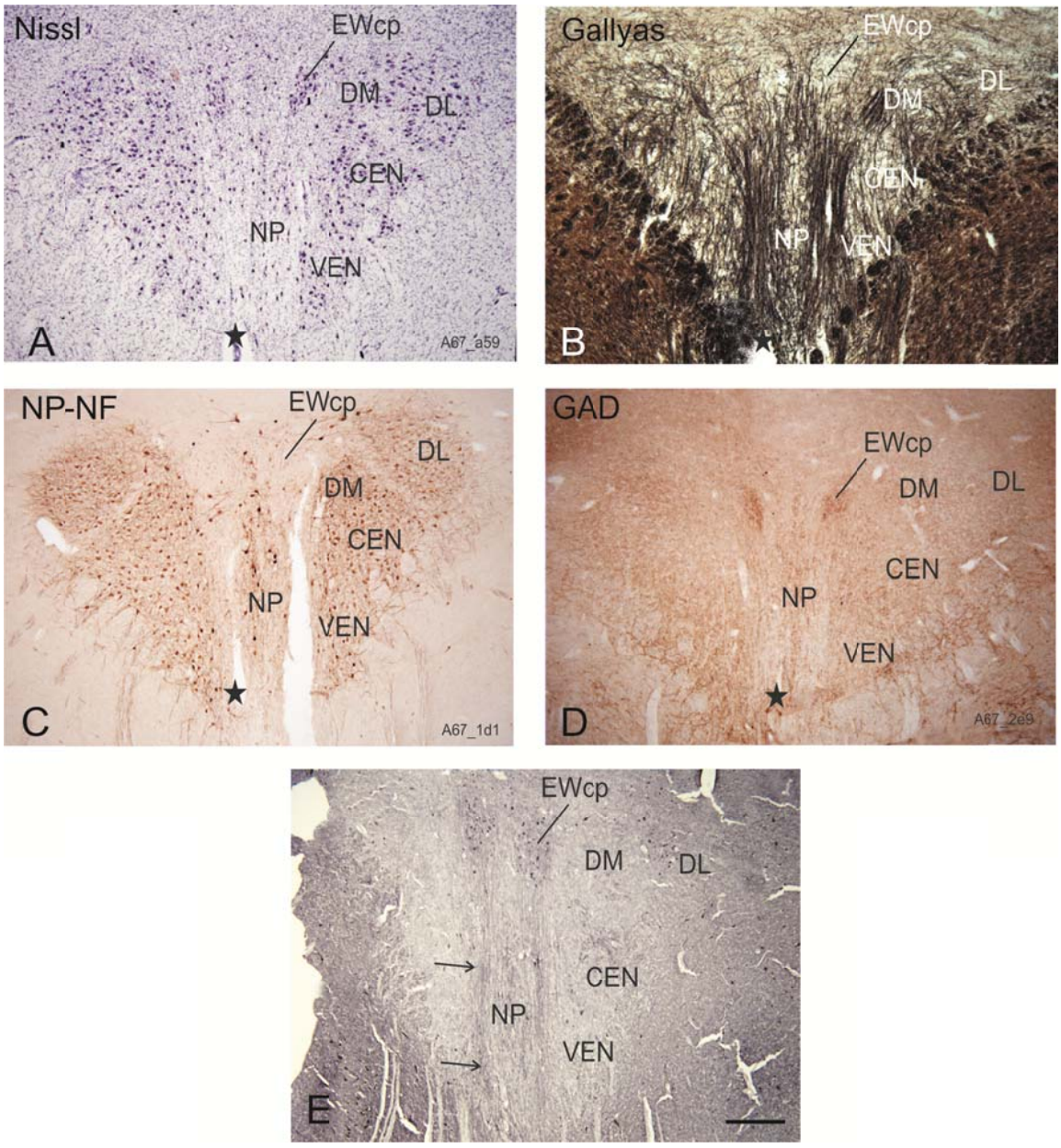

Figure 11. Transverse sections through the oculomotor nucleus at mid-level

Neighbouring transverse sections through the human midbrain at mid-level of the oculomotor nucleus (nIII) with the nucleus of Perlia (NP) at the midline stained for Nissl (A), Gallyas fiber stain (B), non-phosphorylated neurofilaments (NP-NF) in (C), and GAD-immunostaining (D). A blood vessel (star) serves as a landmark. Note that the central projecting Edinger-Westphal nucleus (EWcp) is most densely labelled by GAD-positive puncta (D), whereas the dorsolateral (DL) and ventral subgroup (VEN) show less strong GAD-immunostaining. Note in (E) the calretinin-positive neurons in the EWcp with fibres travelling dorsoventrally (arrows) and the strong CR- positive profiles in the NP. DM= dorsomedial subgroup, LAT= lateral subgroup, MLF = medial longitudinal fascicle. "A modified version of this figure is published in Che Ngwa et al., 2014, Frontiers in Neuroanatomy 8:2"

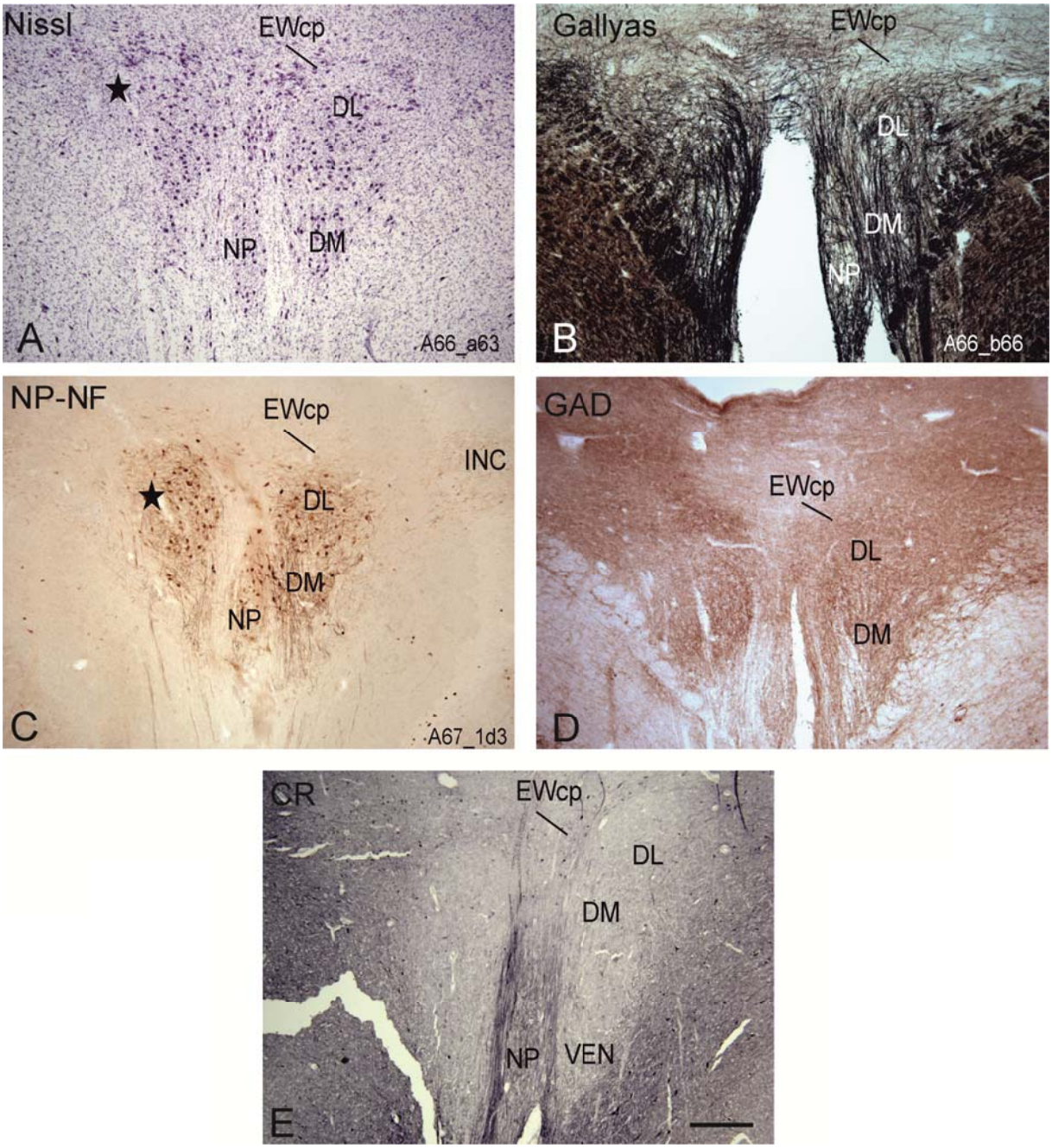

Figure 12. Transverse sections through the nucleus of Perlia
Neighbouring transverse sections through the human brainstem at the rostral plane of the oculomotor nucleus with the Nucleus of Perlia (NP) at the midline stained for Nissl (A), Gallyas fiber stain (B), non-phosphorylated neurofilaments (NP-NF) and GAD-immunostaining (D). A blood vessel (star) serves as a landmark. Note the strong calretinin-positive fibres travelling dorsoventrally enveloping the Nucleus of Perlia (NP), which is covered by numerous CR- positive profiles (E). DM = dorsomedial, DL= dorsolateral subgroup, VEN = ventral group, EWcp = central projecting Edinger Westphal nucleus, INC = interstitial nucleus of Cajal. "A modified version of this figure is published in Che Ngwa et al., 2014, Frontiers in Neuroanatomy 8:2"

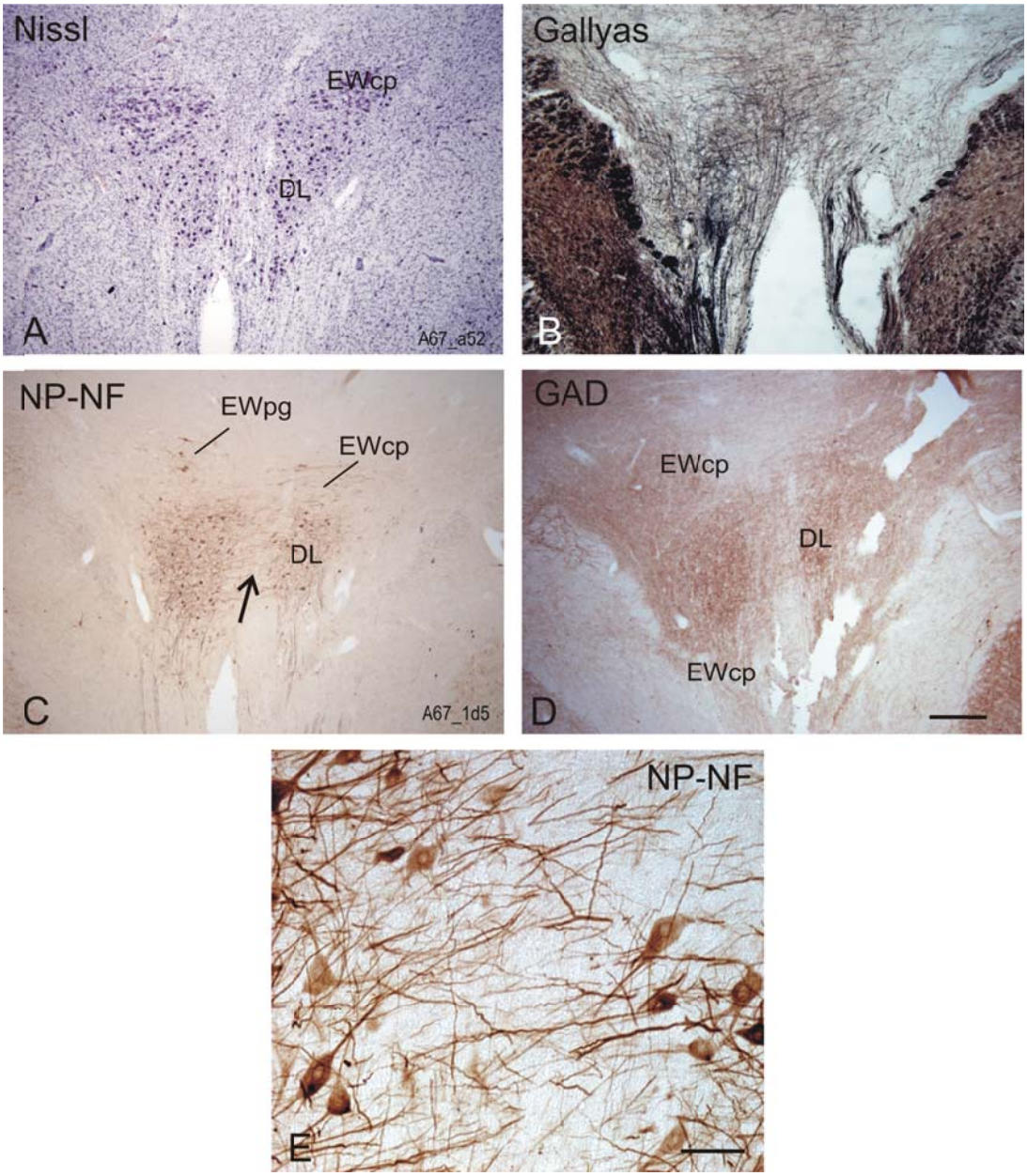

Figure 13. Transverse sections through the rostral oculomotor nucleus
Neighbouring transverse sections through most rostral plane of the oculomotor nucleus stained for Nissl (A), Gallyas fiber stain (B), non-phosphorylated neurofilaments (NP-NF) and GAD-immunostaining (D). As previously described the preganglionic neurons of EWpg express NP-NF, whereas the EWcp not (C). Note that between the dorsolateral subgroups (DL) of both sides numerous NP-NF-positive processes are crossing the midline (C, arrow), more clearly seen in the highpower magnification (E). EWcp = central projecting Edinger Westphal nucleus, EWpg = preganglionic Edinger-Westphal nucleus. "A modified version of this figure is published in Che Ngwa et al., 2014, Frontiers in Neuroanatomy 8:2"

3.3. SEMIQUANTITATIVE ANALYSIS OF GABA AND CALRETININ INPUTS

The semiquantitative analysis of GABA and CR-positive axonal and synaptic profiles was judged at microscopic views of all subgroups in nIII and nIV at high-power magnification (see Figures 14 and 15). The density of GAD- and CR-positive puncta, which represent cut axons and synaptic endings, were judged as either very strong, moderate to strong, or weak. This analysis was accordingly marked in a series of schematic views of nIII and nIV at different caudo-rostral planes (Fig. 16, strong, medium, weak shading). The strongest GAD-input was found to neurons of the EWcp, which densely covered all portions of EWcp (Fig. 16E,G,I). A similar strong GAD-input was found to SO motoneurons in nIV, CEN, LAT, DL, VEN, NP and CCN (Fig. 16A,C, E, G, I), whereas only a weak GAD-input was apparent in the DM subgroup (Fig. 16 C, E, G, I). For CR the strongest input was found around neurons in CCN, NP and CEN (Fig. 16 D, F, H). All other subgroups in the nIII and nIV contained only few CR-profiles most of them representing traversing fibers (Fig. 16 B, D, F, H, K). The EWcp was found to contain CR-positive cell bodies, which are indicated by red dots (Fig. 16 F, 16H, 16K, 16M).

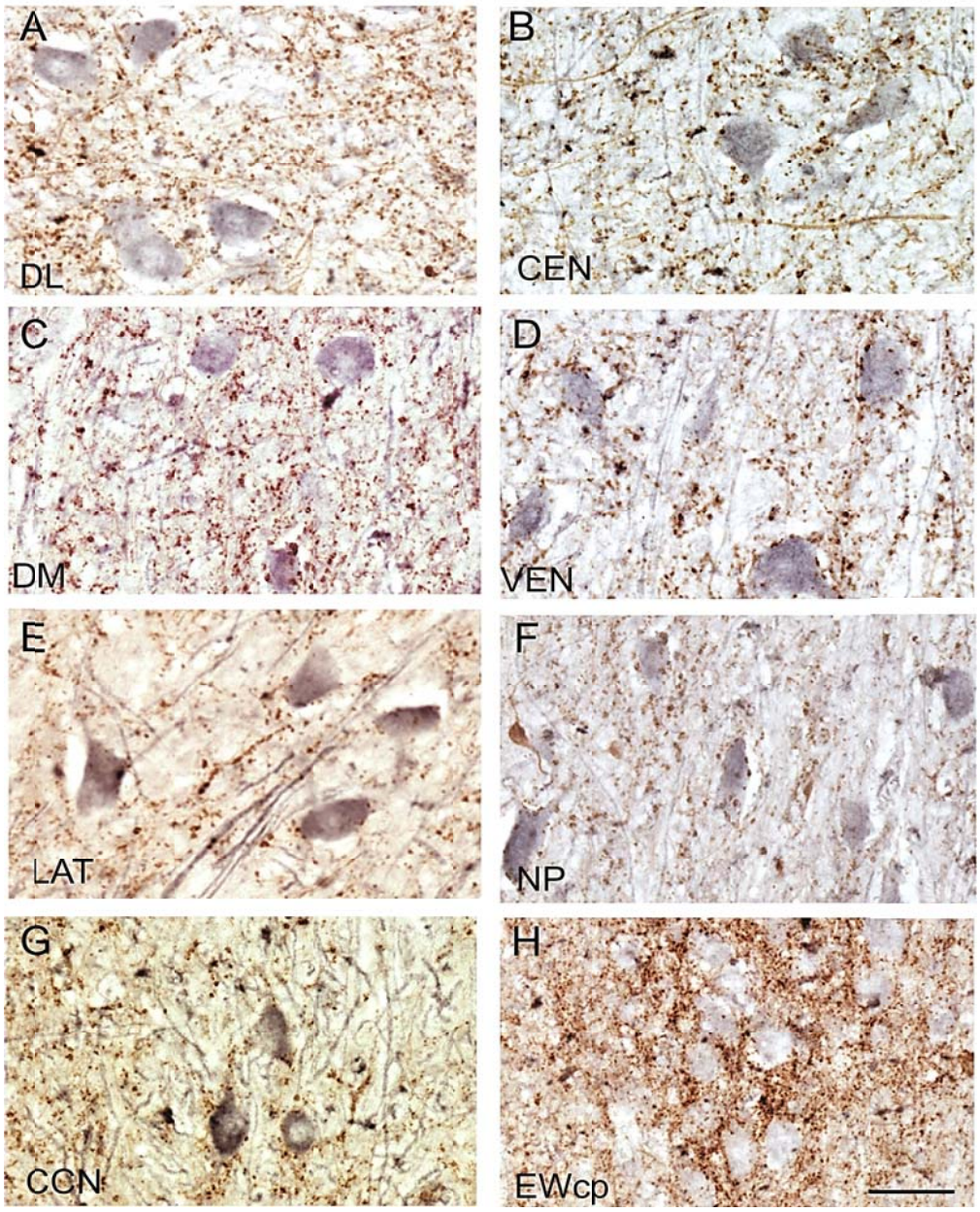

Figure 14. Detailed views of the ChAT- and GAD-immunostaining in the oculomotor nucleus
High-power magnification of transverse sections through the human oculomotor nucleus immunostained for choline acetyltransferase (ChAT) revealing by a black stain and glutamate decarboxylase (GAD) staining in brown. The ChAT-negative central projecting Edinger-Westphal nucleus receives the strongest supply from GAD-positive punctate profiles (H). A similar strong GAD input is found to DL (A), VEN (D), CEN (B), LAT (E), whereas DM and NP is covered by less GAD-positive puncta (C, F). NP= Nucleus of Perlia, DL= Dorsolateral subgroup, DM= dorsomedial subgroup, CEN= central subgroup, VEN= ventral subgroup, LAT= lateral subgroup, CCN= central caudal nucleus. Scale bar A-H: 30µm. " A modified version of this figure is published in Che Ngwa et al., 2014, Frontiers in Neuroanatomy 8:2"

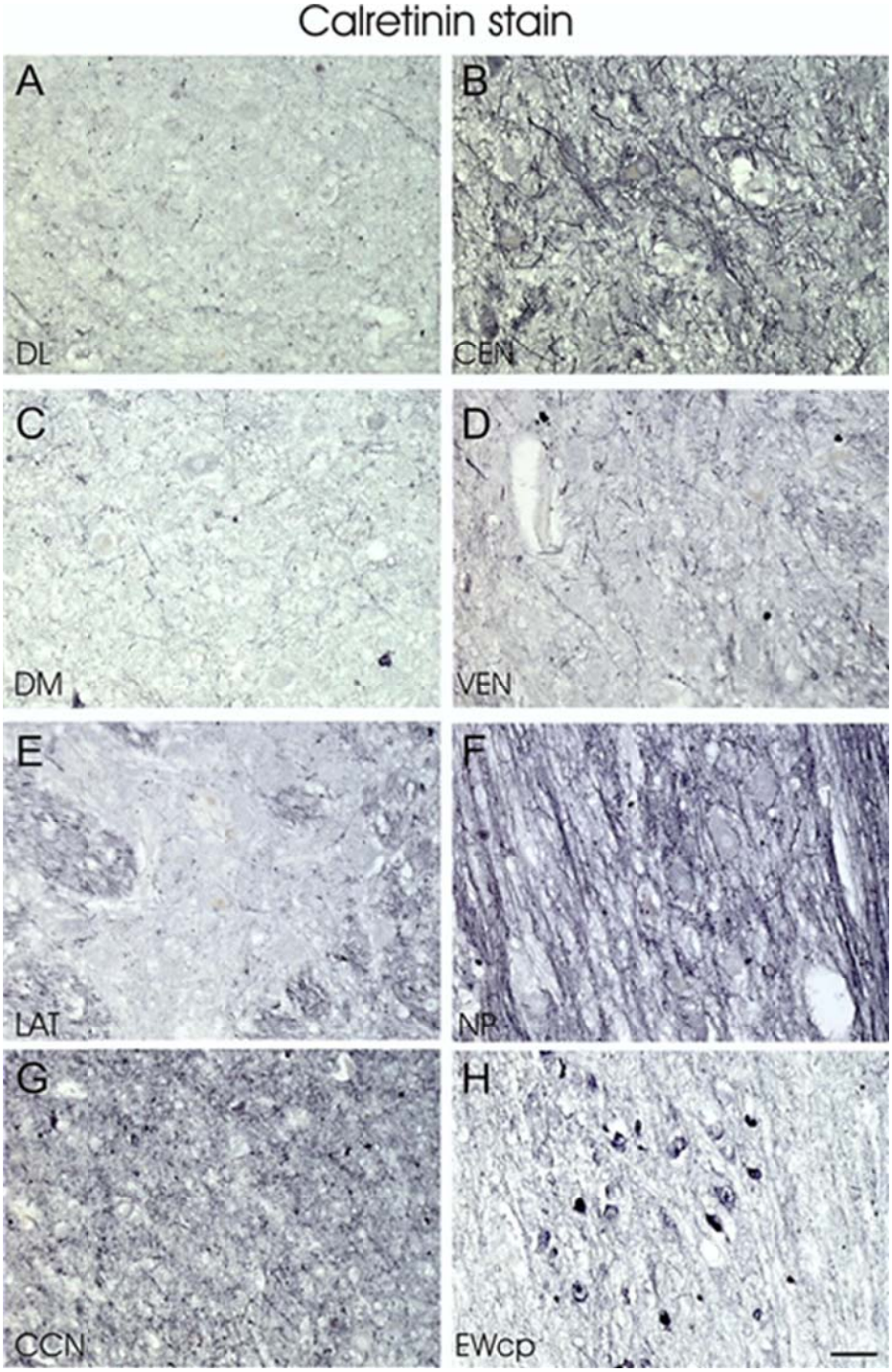

Figure 15. Detailed view of the calretinin-immunostaining in the oculomotor nucleus
High-power magnification of transverse sections through the human oculomotor nucleus immunostained for calretinin (CR). The strongest supply of CR-positive terminals and CR fiber staining is present in the central subgroup (CEN) (B), the nucleus of Perlia (NP) (F), and the central caudal nucleus (G). Only few CR-positive fibers are present in the other oculomotor cell groups (A, C, D, E). The central projecting Edinger-Westphal nucleus contains numerous CR-positive neurons (H). Scale bar A-H: 50µm. "A modified version of this figure is published in Che Ngwa et al., 2014, Frontiers in Neuroanatomy 8:2"

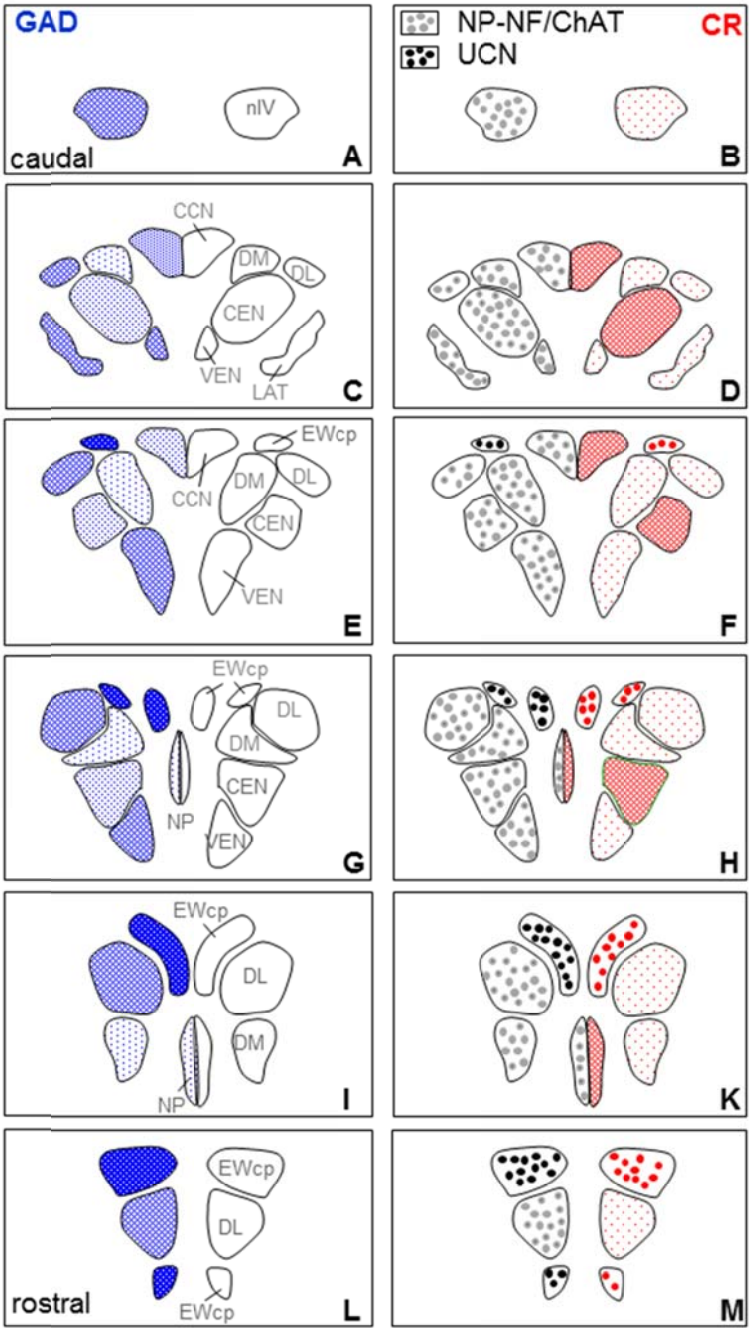

Figure 16. Histochemical properties of subgroups within the human oculomotor nucleus
Schematic caudo-rostral series of transverse sections of the human trochlear and oculomotor nucleus demonstrating the association with glutamate decarboxylase (GAD), non-phosphorylated neurofilaments (NP-NF) and choline acetyltransferase (ChAT), urocortin (UCN) and calretinin (CR) in cell bodies (large dots) or terminals (small dots) in a semiquantitative manner. An extended version including glycinergic inputs is published in Che Ngwa et al., 2014, Frontiers in Neuroanatomy 8:2.

4 DISCUSSION

The present study of the cytoarchitectural characteristics and histochemical properties of the human oculomotor nucleus provides the basis for the identification of the subgroups of individual muscles by comparison with findings in non-human primates based on tract-tracing and studies of the histochemical profile (Büttner-Ennever et al., 2001; Zeeh et al., 2013, 2015). Compared with previous studies, the designation of eye muscle subgroups is unique, and the evidence supporting this version in human is the most rigorous up to date. Based on the present study an updated map of the oculomotor nucleus in human has been developed (Fig. 17) (Che Ngwa et al., 2014).

4.1. HISTOCHEMICAL PROPERTIES OF OCULOMOTOR NUCLEUS SUBGROUPS

4.1.1. CALRETININ

4.1.1.1. Motoneurons for upgaze

As in monkey, a strong CR input was only found in selected groups within nIII, which include the central group (CEN) and the central caudal nucleus (CCN) (Zeeh et al., 2013). Tract-tracer injections into extraocular muscles in monkey have revealed that the motoneurons of the ipsilateral IO and contralateral SR occupy a similar location in the caudal nIII as CEN in human (Spencer and Porter, 1981; Zeeh et al., 2013). Furthermore, both populations, which mediate upward eye movements, are rather mixed with each other, which indicate that they may receive similar inputs (Leigh and Zee, 2015). Since combined immunostaining for CR and GAD in monkey did not show any colocalization within synaptic nerve endings surrounding IO and SR motoneurons, the CR input is considered to be excitatory (Zeeh et al., 2013), given the fact that glycine-positive inputs (the other potential inhibitory transmitter) are only found around MR neurons within nIII (Spencer et al., 1992; Che Ngwa et al., 2014; Zeeh et al., 2015). Tract-tracer injections into nIII and combined immunostaining in monkey revealed three sources of CR-positive afferents: the rostral interstitial nucleus of the medial longitudinal fascicle (RIMLF), the interstitial nucleus of Cajal (INC) and the vestibular Y-group (Ahlfeld et al., 2011). The CR input did also include the CCN, containing the LP motoneurons, which are activated during upward eye movements in a similar way as the SR motoneurons mediating concomitant lid movements during upgaze (Fuchs et al., 1992). Given the fact that the CEN group in the human nIII has similar histochemical characteristics as

upgaze motoneurons in monkey this group is considered as the IO and SR motoneuronal subgroup in human (Che Ngwa et al., 2014). This selective CR-input to IO and SR motoneurons may serve as an anatomical tool to identify the premotor pathways mediating upgaze in human tissue. Based on the work in monkey (Ahlfeld et al., 2011) a recent post-mortem human study revealed that a subpopulation of parvalbumin-positive neurons in the RIMLF expressed CR, which therefore may be considered as premotor up-burst neurons (Adamczyk et al., 2015). As in monkey the CR-positive population in INC may represent excitatory neurons that are involved in the integration of eye-velocity to eye-position signals for upward eye movements transmitted to the SR and IO motoneurons (Adamczyk et al., 2015). In addition, the Y-group is another possible source of CR-positive input as indicated by the presence of CR-expressing neurons in human (Adamczyk et al., 2015). In monkey electrical stimulation of the Y-group was shown to induce excitatory signals in the IO and SR motoneurons resulting in slow upward eye movements (Chubb and Fuchs, 1982; Sato and Kawasaki, 1987).

4.1.1.2. Function of Calretinin

So far the functional significance for the selective expression of CR in premotor upgaze pathways is unclear. As a calcium-binding protein it may be involved in buffer function controlling the concentration of free calcium or in calcium sensoring (Schwaller, 2014). Another calcium-binding protein, parvalbumin, has been found in many fast-firing highly active neurons of the oculomotor system, which includes motoneurons, saccadic premotor neurons in the RIMLF and INC and omnipause neurons (for review: Horn, 2006; Horn and Adamczyk, 2011). No such association with specific properties is known for CR-positive neurons. Suggested functions of CR are a role in neuron protection, synaptic plasticity or a role in the regulation of neuronal excitability (for review: Schwaller, 2014).

4.1.2. GLUTAMATE DECARBOXYLASE

Unlike in monkey a considerable GABAergic input was found to all subgroups of eye muscle motonuclei in human. Complimentary work indicated that the human DL and VEN groups were specifically associated with glycinergic markers as found for the MR subgroups in monkey (Spencer and Baker, 1992; Zeeh et al., 2015). Therefore the VEN is considered as the MR A-group and the DL as the MR B-group (Che Ngwa et al., 2014). Whereas in monkey the MR subgroups receive only a moderate GABAergic input (Zeeh et al., 2015), in human a very strong supply by GABAergic terminals was noted. Since a more or less strong GABA

input was found to all nIII subnuclei, this property was not very helpful for the delineation of the subgroups by its own, but only in combination with the other markers for CR and glycine (Che Ngwa et al., 2014).

In monkey and cat a GABAergic input to the motoneurons of vertically pulling eye muscles was found to arise from neurons in the vestibular nucleus mediating the vestibulo-ocular reflex (De la Cruz et al., 1992; Wentzel et al., 1996; Highstein and Holstein, 2006). Further sources of GABAergic afferents are premotor neurons in the INC (Horn et al., 2003), which correspond to the finding of inhibitory postsynaptic potentials in nIII and nIV observed after INC stimulation (Schwindt et al., 1974; Sugiuchi et al., 2013). It is unclear, why in human the histochemical pattern for GABAergic markers in nIII differs from that of non-human primates. However it is in line with the observation that also the human abducens nucleus (nVI), which mediates horizontal eye movements as well, receives a rich supply from GABAergic afferents, unlike in monkey (Spencer et al., 2003; Dombi, Dissertation LMU, 2014). A possible source of a GABAergic input to the MR subgroups in human is the central mesencephalic reticular formation (CMRF) (Büttner-Ennever and Horn, 2014). This area is interconnected with the superior colliculus and the premotor horizontal gaze center in the pontine reticular formation (Cohen, 1984; Chen et al., 2000). The activity of neurons in the CMRF is correlated with horizontal and vertical saccades (Waitzman et al., 2002), but recent studies indicated a direct projection to neurons involved in the near response, consisting of convergence, pupillary constriction and lens accommodation. Preliminary data from tract-tracing experiments in monkey revealed that many terminals originating from the CMRF and targeting MR motoneurons are GABAergic (Bohlen et al., 2015). It is well possible that this near response system used for fixating near visual targets is much more evolved in human (Leigh and Zee, 2015).

4.2. Histochemical properties of perioculomotor Cell groups

4.2.1. Nucleus of Perlia

Contrary to Le Gros Clark (1926) and in agreement with Brouwer`s postulation in primates and insectivores the spindle shaped nucleus of Perlia (NP) is a consistent entity lying in the middle third of the oculomotor nucleus, and it is present in 80% of human (see Büttner-Ennever and Horn 2014). Based on the coincidence of its appearance in evolution with the frontal eye position enabling convergent eye movements a synergistic function to MR motoneurons was anticipated for NP (Adler, 1933). The NP was not found in other animals.

Reports about a group of retrogradely labelled neurons at the midline between both nIII after tract-tracer injections into the ciliary ganglion in monkey must be interpreted with caution (Burde and Williams, 1989). These neurons are likely to represent the MIF motoneurons of IO and SR of the medial S-group, which may have taken up the tracer (discussed in Horn et al. 2008). So far there is more evidence that the neurons of NP exhibit features of twitch SIF motoneurons, e.g. expression of ChAT and NP-NF and ensheathing by perineuronal nets (present study; Horn et al., 2008; Che Ngwa et al., 2014). A complete new finding of the present study is the association of NP with CR-positive puncta and fibres suggesting a CR input to this subgroup (Che Ngwa et al., 2014). Considering the findings on a selective CR input to those motoneurons involved in upgaze in monkey (Zeeh et al., 2013) and presumably also in man, the NP may represent SR SIF motoneurons that have been separated from the adjacent main nIII by dorsoventrally travelling axons (Horn et al., 2008; Büttner-Ennever and Horn, 2014; Che Ngwa et al., 2014).

4.2.2. EDINGER-WESTPHAL NUCLEUS

Traditionally the Edinger-Westphal nucleus is considered as the location for the preganglionic neurons of the ciliary ganglion controlling the lens and the sphincter pupillae muscle. However several reports showed that this is true only in monkey and avian, whereas in all other species studied so far - including human - the EW consists of neurons containing the neuropeptide urocortin (Horn et al., 2009). This urocortin-positive group has been identified in other species as well and was found to project to other central targets subserving different functions in stress reaction or water and food intake (Skelton et al., 2000; Kozicz et al., 2001). To avoid confusion between scientists working on the different systems a new nomenclature was introduced for the EW: now the term “EWcp” refers to the centrally projecting non-cholinergic neurons, whereas “EWpg” refers to the cholinergic parasympathetic preganglionic neurons of the ciliary ganglion (Kozicz et al., 2011; Büttner-Ennever and Horn, 2014). As described earlier the EWcp forms a group of small tightly packed neurons dorsal to the nIII at caudal levels, which do not express NP-NF or ChAT- immunostaining. At rostral planes through nIII a ventral portion of EWcp was visible. The present study revealed that the EWcp received the densest supply from GABAergic terminals, whose source is not known, yet. In addition it contained several CR-positive neurons that formed a largely independent population from urocortin-positive neurons shown by comparison of neighbouring 5µm sections stained for CR and urocortin, respectively (Che Ngwa et al., 2014).

4.2.1. TWITCH- AND NON-TWITCH MOTONEURONS

It has been well established that extraocular muscles contain at least six different muscle fiber types, which can be divided into two main categories based on their innervation and contraction properties: singly-innervated twitch muscle fibers (SIF) and multiply-innervated non-twitch muscle fibers (MIF) (for review: Spencer and Porter, 2006). Tract-tracing experiments revealed that the motoneurons of MIFs are located in the periphery of the motonuclei (for review: Büttner-Ennever 2006). In monkey the MIF motoneurons of IR and MR are located in the C-group dorsomedial to nIII and those of IO and SR in the S-group between the both nIII (Büttner-Ennever et al., 2001). Both motoneuron groups differ also in their histochemical properties: SIF motoneurons within nIII express NP-NF immunoreactivity and are ensheathed by perineuronal nets, whereas MIF motoneurons lack these markers (Eberhorn et al., 2005; Eberhorn et al., 2006). Using these histochemical properties putative MIF motoneurons have been described around the medial aspects of nIII in human as well, but the MIF motoneurons could not be allocated to specific extraocular muscles, yet (Horn et al., 2008). A recent immunohistochemical study on transmitter inputs to nIII in monkey with emphasis on MIF and SIF motoneurons did not reveal significant differences in transmitter inputs to both populations, except for vesicular glutamate transporter 1, which was found only at MR MIF motoneurons (Zeeh et al., 2015), but this antibody has not been used in the present study on human tissue. Therefore the proposed oculomotor map in human applies only to the SIF motoneurons of individual extraocular muscles. Further studies are necessary to extend the map to include the location of MIF motoneurons.

4.3. MAP OF THE OCULOMOTOR NUCLEUS IN HUMANS

Different methods including stimulation, retrograde degeneration, tract tracing and immunohistochemical methods have been used in previous animal studies describing the representation of the extraocular muscle within nIII in various vertebrate species (for review: Evinger, 1988; Büttner-Ennever, 2006). Degeneration or tract-tracing studies in monkeys (Warwick, 1953; Augustine et al., 1981; Büttner-Ennever and Akert, 1981; Porter et al., 1983; Sun and May, 1993), cats (Gacek, 1974; Akagi, 1978; Miyazaki, 1985), rabbit (Akagi, 1978; Shaw and Alley, 1981; Murphy et al., 1986), rat (Glicksman, 1980; Oda, 1981; Labandeira-Garcia et al., 1983), and guinea pig (Gomez-Segade and Labandeira-Garcia, 1983; Evinger et al., 1987), have shown that the motoneurons of nIII are arranged in subgroups. In general the

arrangement of subgroups of individual eye muscles follow a similar pattern found in all vertebrate species (for review: Evinger, 1988; Büttner-Ennever, 2006): Motoneurons of the oculomotor nucleus innervate the ipsilateral MR, IR and IO, and the contralateral SR. The rostro-caudal arrangement of motoneuronal groups starts with the IR, followed by MR, IO and SR, whereas in rodents the LP motoneurons are located within the contralateral nIII, they form an unpaired separate central caudal nucleus in cat and primates including human (Evinger, 1988; Porter et al., 1989; Horn, 2006).

The first anatomical description of nIII was published by Stilling (1846). Later a partition into a dorsal and ventral portion of nIII was described. The presence of decussating axons was first noted by Von Gudden (1881; for review: Warwick, 1953). The work of Warwick, who resected extraocular muscles in monkey and plotted the neurons undergoing chromatolysis provided a map of the non-human primate nIII (Warwick, 1953), which is still being used in textbooks. The tract-tracing methods, which were introduced in the late 70s, basically confirmed the topographical arrangement of motoneuronal groups in nIII of monkey (Büttner-Ennever 2006). However, in this species for the first time the presence of two motoneuron groups for the MR was described: the ventral A-group and the dorsolateral circular B-group (Büttner-Ennever and Akert, 1981; Porter et al., 1983; Büttner-Ennever, 2006). Up to date no differences in the innervation targets, morphology, histochemistry or afferent inputs have been found between the A- and B-group, and the function of the two-fold MR representation remains unclear (Spencer et al., 1992; Büttner-Ennever et al., 2001; Wasicky et al., 2004; Erichsen et al., 2013; Zeeh et al., 2015). Based on the similar GAD-staining pattern in the DL and VEN group together with the finding of a glycine input to these two groups in the human nIII (Che Ngwa et al., 2014) strong evidence is provided that the MR subgroups are similarly organized in human. Accordingly the DL corresponds to the B-group of monkey nIII and VEN to the A-group (Fig. 17).

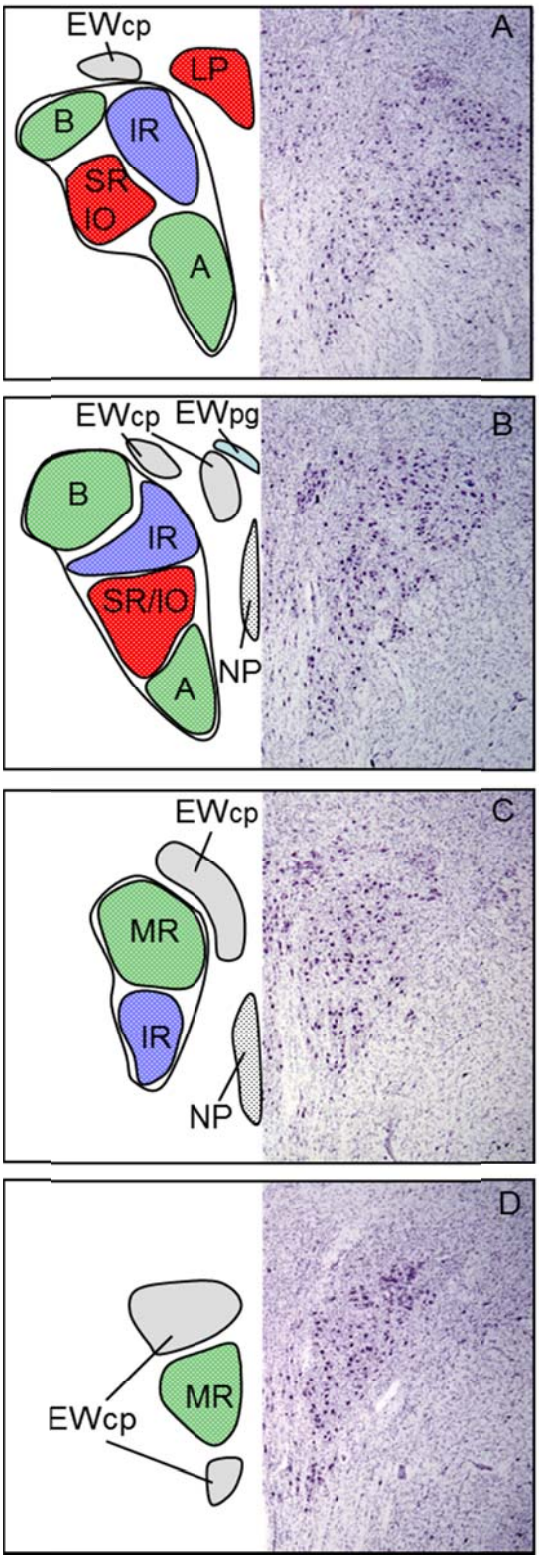

Figure 17. Proposed map of the human oculomotor nucleus
Summary of the identified oculomotor subgroups from cytoarchitecture (on the right) and the proposed correlation with subgroups of motoneurons of individual eye muscles (on the left) based on the histochemical data. (From Che Ngwa et al. 2014; Frontiers in Neuroanatomy 8: 2)

5 CONCLUSION

The present study provides a topographical map of the motoneurons in the human oculomotor nucleus, which is not only based on comparison with the location of the respective motoneuronal pools in monkey based on tract-tracing, but on the different histochemical properties of premotor afferents (Fig. 17). It should be pointed out that the proposed topographical map applies to the motoneurons within the oculomotor nucleus supplying singly-innervated twitch muscle fibers (Che Ngwa et al., 2014). This map has yet to be extended by the location of the peripheral non-twitch motoneurons supplying multiply-innervated muscle fibers of individual eye muscles. A striking observation is the selective CR input to SR and IO motoneurons, which may help to identify premotor pathways involved in upgaze (Che Ngwa et al., 2014; Adamczyk et al., 2015) and to study these pathways in post-mortem studies on cases with vertical gaze deficits, e.g. progressive supranuclear palsy or Niemann-Pick disease (Chen et al., 2010; Strupp et al., 2014). The exact knowledge of the location of the motoneuron subgroups of individual eye muscles in human will help to localize lesions more accurately in MRI scans and correlate them to clinical findings (Leigh and Zee, 2015). Furthermore the present work on transmitter inputs to individual eye muscle subgroups will form the basis for post-mortem studies of afferent inputs to nIII in cases with known eye-movement deficits.

6 REFERENCES

Adamczyk C, Strupp M, Jahn K, Horn AKE (2015) Calretinin as a marker for premotor neurons involved in upgaze in human brainstem. Front Neuroanat 9. doi: 10.3389/fnana.2015.00153

Adler A (1933) Zur Lokalisation des Konvergenzzentrums und der Kerne der glatten Augenmuskeln. Zeits f Neurol Psychiat 145:186-207.

Ahlfeld J, Mustari M, Horn AKE (2011) Sources of calretinin inputs to motoneurons of extraocular muscles involved in upgaze. Ann N Y Acad Sci 1233:91 - 99.

Akagi Y (1978) The localization of the motor neurons innervating the extraocular muscles in the oculomotor nuclei of the cat and rabbit, using horseradish peroxidase. J Comp Neurol 181:745-761.

Andressen C, Blümcke I, Celio MR (1993) Calcium-binding proteins - selective markers of nerve cells. Cell Tiss Res 271:181-208.

Augustine JR, Deschamps EG, Ferguson JGJ (1981) Functional organization of the oculomotor nucleus in the baboon. Amer J Anat 161:393-403.

Baker KG (1992) A comtenporary view of the phylogenetic history of eye muscles and motoneurons. In: Shimazu H, Shinoda Y, eds. Tokyo / Basel: Japan Scientific Societies Press / Karger. p 3-19.

Bender MB, Weinstein EA (1943) Functional representation in the oculomotor and trochlear nuclei. Arch Neur Psych 49:98-106.

Bernheimer S (1897) Experimentelle Studien zur Kenntniss der Innervation der inneren und äusseren vom Oculomotorius versorgten Muskeln des Auges. Arch f Ophthalmol 44:481-525.

Bohlen MO, Warren S, May PJ (2015) A central mesencephalic reticular formation projection to the supraoculomotor area in macaque monkeys. Brain Struct Funct. doi:10.1007/s00429-015-1039-2

Brouwer B. 1918. Klinisch-anatomische Untersuchung über den Oculomotoriuskern. Z Ges Neurol Psychiat 40:152-193.

Bruce G, Wainer BH, Hersh LB (1985) Immunoaffinity purification of human choline acetyltransferase: comparison of the brain and placental enzymes. J Neurochem 45:611-620.

Büttner U, Büttner-Ennever JA (2006) Present concepts of oculomotor organization. Prog Brain Res 151:1-42.

Büttner-Ennever JA (2006) The extraocular motor nuclei: organization and functional neuroanatomy. Prog Brain Res 151:95-125.

Büttner-Ennever JA, Akert K (1981) Medial rectus subgroups of the oculomotor nucleus and their abducens internuclear input in the monkey. J Comp Neurol 197:17-27.

Büttner-Ennever JA, Horn AKE, Scherberger H, D'Ascanio P (2001) Motoneurons of twitch and nontwitch extraocular muscle fibers in the abducens, trochlear, and oculomotor nuclei of monkeys. J Comp Neurol 438:318-335.

Büttner-Ennever JA, Horn AKE (2014) Olszewski and Baxter's Cytoarchitecture of the Human Brainstem, 3rd edition, Karger, Basel.

Burde RM, Williams F. 1989. Parasympathetic nuclei. Brain Res 498:371–375.

Chen B, May PJ (2000) The feedback circuit connecting the superior colliculus and central mesencephalic reticular formation: a direct morphological demonstration. Exp Brain Res 131:10-21.

Chen AL, Riley DE, King SA, Joshi AC, Serra A, Liao K, Cohen ML, Otero-Millan J, Martinez-Conde S, Strupp M, Leigh RJ (2010) The disturbance of gaze in progressive supranuclear palsy (PSP): implications for pathogenesis. Front Neurol 1.

Cohen B, Büttner-Ennever JA (1984) Projections from the superior colliculus to a region of the central mesencephalic reticular formation (cMRF) associated with horizontal saccadic eye movements. Exp Brain Res 57:167-176.

Che Ngwa E, Zeeh C, Messoudi A, Büttner-Ennever JA, Horn AKE (2014) Delineation of motoneuron subgroups supplying individual eye muscles in the human oculomotor nucleus. Front Neuroanat 8.

Chubb MC, Fuchs AF (1982) Contribution of y group of vestibular nuclei and dentate nucleus of cerebellum to generation of vertical smooth eye movements. J. Neurophysiol. 48, 75–99.

Cooper ERA (1946) The development of the nuclei of the oculomotor and trochlear nerves (somatic efferent column). Brain 69:50-57.

Cooper ERA (1947) The trochlear nerve in the human embryo and foetus. Br J Ophthalmol 31:257-275.

De la Cruz RR, Pastor AM, Martinez-Guijarro FJ, Lopez-Garcia C, Delgado-García JM) 1992) Role of GABA in the extraocular motor nuclei of the cat: a postembedding immunocytochemical study. Neuroscience 51:911-929.

Donzelli R, Marinkovic l, Brigante L, Nikodijevic I, Maiuri F, De Divitiis O (1998) The oculomotor nuclear complex in humans. Microanatomy and clinical significance. Surg Radiol Anat 19:7-12.

Eberhorn AC, Ardelenanu P, Büttner-Ennever JA, Horn AKE (2005) Histochemical differences between motoneurons supplying multiply and singly innervated extraocular muscle fibers. J Comp Neurol 491:352-366.

Eberhorn AC, Büttner-Ennever JA, Horn AKE (2006) Identification of motoneurons innervating multiply- or singly-innervated extraocular muscle fibres in the rat. Neuroscience 137:891-903.

Edinger L (1885) Über den Verlauf der centralen Hirnnervenbahnen mit Demonstrationen von Präparaten. Arch Psychiat Nervenkr 16:858-859.

El-Hassni M, Bennis M, Rio JP, Reperant J (2000) Localization of motoneurons innervating the extraocular muscles in the chameleon (chamaelo chameleon). Anat Embryol 201:63-74.

Erichsen JT, Wright NF, May PJ (2013) The morphology and ultrastructure of medial rectus subgroup motoneurons in the macaque monkey. J Comp Neurol 522:626-624

Evinger C (1988) Extraocular motor nuclei: location, morphology and afferents. In: Büttner-Ennever JA, ed. Rev. Oculomot. Res. Amsterdam; New York; Oxford: Elsevier. p 81-117.

Evinger C, Graf WM, Baker R (1987) Extra- and intracellular HRP analysis of the organization of extraocular motoneurons and internuclear neurons in the guinea pig and rabbit. J Comp Neurol 262:429-445.

Fuchs AF, Becker W, Ling L, Langer TP, Kaneko CR (1992) Discharge patterns of levator palpebrae superioris motoneurons during vertical lid and eye movements in the monkey. J Neurophysiol 68:233-243.

Gacek RR (1974) Localization of neurons supplying the extraocular muscles in the kitten using horseradish peroxidase. Expl Neurol 44:381-403.

Gaszner B, Csernus V, Kozicz T (2004) Urocortinergic neurons respond in a differentiated manner to various acute stressors in the Edinger-Westphal nucleus in the rat. J Comp Neurol 480:170-179.

Giardino WJ, Cocking DL, Kaur S, Cunningham CL, Ryabinin AE (2011) Urocortin-1 within the centrally-projecting Edinger-Westphal nucleus is critical for ethanol preference. PLoS ONE 6:e26997.

Glicksman MA (1980) Localization of motoneurons controlling the extraocular muscles of the rat. Brain Res 188:53-62.

Gomez-Segade LA, Labandeira-Garcia JL (1983) Location and quantitative analysis of the motoneurons innervating the extraocular muscles of the guinea-pig, using horseradish peroxidase (HRP) and double or triple labelling with fluorescent substances. J Hirnforsch 24:613-626.

Highstein SM, Holstein GR (2006) The anatomy of the vestibular nuclei. Prog Brain Res 151:157-203.

Horn AK, Eberhorn A, Härtig W, Ardelenanu P, Messoudi A, Büttner-Ennever JA (2008) Perioculomotor cell groups in monkey and man defined by their histochemical and functional properties: reappraisal of the Edinger-Westphal nucleus. J Comp Neurol 507:1317-1335.

Horn AK, Schulze C, Radtke-Schuller S (2009) The Edinger-Westphal nucleus represents different functional cell groups in different species. Ann N Y Acad Sci 1164:45-50.

Horn AKE. 2006. The reticular formation. Prog Brain Res 151:127-155.

Horn AKE, Adamcyzk C (2011) Reticular Formation - Eye Movements, Gaze and Blinks. Mai JK, Paxinos, G. ed: Academic Press.

Horn AKE, Helmchen C, Wahle P (2003) GABAergic neurons in the rostral mesencephalon of the Macaque monkey that control vertical eye movements. Ann N Y Acad Sci 1004:19-28.

Isomura G (1981) Comparative anatomy of the extrinsic ocular muscles in vertebrates. Anat Anz 150:498-515.

Jiao Y, Sun Z, Lee T, Fusco FR, Kimble TD, Meade CA, Cuthbertson S, Reiner A (1999) A simple and sensitive antigen retrieval method for free-floating and slide-mounted tissue sections. J Neurosci Meth 93:149-162.

Kozicz T, Bittencourt JC, May PJ, Reiner A, Gamlin PDR, Palkovits M, Horn AKE, Toledo CAB, Ryabinin AE (2011) The Edinger-Westphal nucleus: A historical, structural, and functional perspective on a dichotomous terminology. J Comp Neurol 519:1413-1434.

Kozicz T, Min A, Arimura A. 2001. The activation of urocortin immunoreactive neurons in the Edinger-Westphal nucleus following acute pain stress in rats. Stress 4:85-90.

Kuypers HG, Catsman-Berrevoets CE, Padt RE (1977) Retrograde anoxal transport of fluorescent substances in the rat's forebrain. Neurosci Lett 6:127-133.

Labandeira-Garcia JL, Gomez-Segade LA, Nunez JMS (1983) Localisation of motoneurons supplying the extra-ocular muscles of the rat using horseradish peroxidase and fluorescent double labelling. J Anat 137:247-261.

Le Gros Clark WE (1926) The mammalian oculomotor nucleus. J Anat 60:426-448.

Leigh RJ, Zee DS. 2015. The Neurology of Eye Movements. Leigh RJ, Zee DS, eds. New York: Oxford University Press. 3-762 p.

Lienbacher K, Mustari M, Ying HS, Büttner-Ennever JA, Horn AKE (2011) Do palisade endings in extraocular muscles arise from neurons in the motor nuclei? IOVS 52:2510-2519.

Mann IC (1927) The developing third nerve nucleus in human embryos. J Anat 61:424-438.

McDougal D, Gamlin PD (2015) Autonomic control of the eye. Comprehensive Physiology 5.

Matesz C (1990) Development of the oculomotor and trochlear nuclei in the Xenopus toad. Neuroscience Letters 116:1-6.

Mesulam MM (1978) Tetramethyl benzidine for horseradish peroxidase neurohistochemistry: a non-carcinogenic blue reaction-product with superior sensitivity for visualizing neural afferents and efferents. J Histochem Cytochem 26:106-117.

Miyazaki S (1985) Location of motoneurons in the oculomotor nucleus and the course of their axons in the oculomotor nerve. Brain Research 348:57-63.

Muñoz M, González A (1995) The trochlear nucleus of the frog Rana ridibunda: Localization, morphology and ultrastructure of identified motoneurons. Brain Res Bull 36:433-441.

Murphy EH, Garone M, Tashayyod D, Baker RB (1986) Innervation of extraocular muscles in the rabbit. J Comp Neurol 254:78-90.
Naujoks-Manteuffel C, Manteuffel G, Himstedt W (1986) Localization of motoneurons innervating the extraocular muscles in Salamandra salamandra L. (Amphibia, Urodela). J Comp Neurol 254:133-141.
Oda Y (1981) Extraocular muscles and their relationship to the accessory abducens nucleus in rats as studied by the horseradish peroxidase method. Folia Anat Jpn 58:43-54.
Olszewski J, Baxter D (1982) Cytoarchitecture of the human brain stem. Basel, Sydney: S.Karger.
Pearson AA (1943) Trochlear nerve in human fetuses. J Comp Neurol 78:29-43.
Pearson AA (1944) The oculomotor nucleus in the human fetus. J Comp Neurol 80:47-63.
Perlia D (1889) Die Anatomie des Oculomotoriuscentrum beim Menschen. Arch f Ophthalmol 35:287-308.
Porter JD, Baker RS (1992) Prenatal morphogenesis of primate extraocular muscle: neuromuscular junction formation and fiber type differentiation. IOVS 33:657-670.
Porter JD, Burns LA, May PJ (1989) Morphological substrate for eyelid movements: innervation and structure of primate levator palpebrae superioris and orbicularis oculi muscles. J Comp Neurol 287:64-81.
Porter JD, Guthrie BL, Sparks DL (1983) Innervation of monkey extraocular muscles: localization of sensory and motor neurons by retrograde transport of horseradish peroxidase. J Comp Neurol 218:208-219.
Romeis B (2010) Mikroskopische Technik , Mulisch M, Welsch U, eds, 18th ed, Spektrum Akademischer Verlag,
Ryabinin AE, Tsivkovskaia NO, Ryabinin SA. 2005. Urocortin 1-containing neurons in the human Edinger-Westphal nucleus. Neuroscience 134:1317-1323.
Sato Y, Kawasaki T. 1987. Organization of maculo-ocular pathways via y-group nucleus and its relevance to cerebellar flocculus in cats. Physiologist 30:S77-S80.
Schmidtke K, Büttner-Ennever JA (1992) Nervous control of eyelid function - a review of clinical, experimental and pathological data. Brain 115:227-247.
Schwaller B (2014) Calretinin: from a “simple” Ca2+ buffer to a multifunctional protein implicated in many biological processes. Front Neuroanatomy 8.
Schwindt PC, Precht W, Richter A (1974) Monosynaptic excitatory and inhibitory pathways from medial midbrain nuclei to trochlear motoneurons. Exp Brain Res 20:223-238.
Shaw MD, Alley KE (1981) Generation of the ocular motor nuclei and their cell types in the rabbit. J Comp Neurol 200:69-82.
Siebeck R, Kruger P (1955) [The histological structure of the extrinsic ocular muscles as an indication of their function]. Von Graefes Arch Ophthalmol 156:636-652.
Skelton KH, Owens MH, Nemeroff CB (2000) The neurobiology of urocortin. Reg Pept 93:85-92.
Sohal GS, Knox TS, Allen JCJ, Arumugam T, Campbell LR, Yamashita T (1985) Development of the trochlear nucleus in quail and comparative study of the trochlear nucleus, nerve, and innervation of the superior oblique muscle in quail, chick, and duck. J Comp Neurol 239:227-236.
Spencer RF, Wenthold RJ, Baker R (1989) Evidence for glycine as an inhibitory neurotransmitter of vestibular, reticular, and prepositus hypoglossi neurons that project to the cat abducens nucleus. J Neurosci 9:2718-2736.
Spencer RF, Baker R (1992) GABA and glycine as inhibitory neurotransmitters in the vestibulo-ocular reflex. Ann N Y Acad Sci 656:602-611.
Spencer RF, Porter JD (1981) Innervation and structure of extraocular muscles in the monkey in comparison to those of the cat. J Comp Neurol 198:649-665.

Spencer RF, Porter JD (2006) Biological organization of the extraocular muscles. Prog Brain Res 151:43-80.
Spencer RF, Wang SF, Baker R (2003) The pathways and functions of GABA in the oculomotor system. Prog Brain Res 90:307-331.
Stilling,B (1846) Dis quisitiones destructure et functionibus cerebri. *Jenae:sumt. F.Maukii.T.* 1, 36.
Straka H, Gilland E, Baker R (1998) Rhombomeric organization of brainstem motor neurons in larval frogs. Biol Bull 195:220-222.
Straka H, Baker R, Gilland E (2001) Rhombomeric organization of vestibular pathways in larval frogs. J Comp Neurol 437:42-55.
Strupp M, Kremmyda O, Adamczyk C, Böttcher N, Muth C, Yip CW, Bremova T (2014) Central ocular motor disorders, including gaze palsy and nystagmus. J Neurol 261:542-558.
Sturrock RR (1991) Stability of motor neuron number in the oculomotor and trochlear nuclei of the ageing mouse brain. J Anat 174:125-129.
Sugiuchi Y, Takahashi M, Shinoda Y (2013) Input-output organization of inhibitory neurons in the interstitial nucleus of Cajal projecting to the contralateral trochlear and oculomotor nucleus. J Neurophysiol 110:640-657.
Sun W, May PJ (1993) Organization of the extraocular and preganglionic motoneurons supplying the orbit in the lessor galago. The Anat Rec 237:89-103.
Van der Werf F, Aramideh M, Ongerboer de Visser BW, Baljet B, Speelman JD, Otto JA (1997) A retrograde double fluorescent tracing study of the levator palpebrae superioris muscle in the cynomolgus monkey. Exp Brain Res 113:174-179.
Vaughan J, Donaldson C, Bittencourt JC, Perrin MH, Lewis K, Sutton S, Chan R, Turnbull A, Lovejoy D, Rivier C, Rivier J, Sawchenko PE, Vale W (1995) Urocortin, a mammalian neuropeptide related to fish urotensin I and to corticotropin-releasing factor. Nature 378:287-292.
Vijayashankar N, Brody H (1977) Aging in the human brain stem. A study of the nucleus of the trochlear nerve. Acta Anat. 99:169-172.
Von Gudden B (1881) Über den Tractus peduncularis traversus. Arch Psychiat Nervenkr 2:364-366.
Waitzman DM, Van Horn MR, Cullen KE (2008) Neuronal evidence for individual eye control in the primate cMRF. Prog Brain Res 171:143-150.
Warwick R (1953) Representation of the extraocular muscles in the oculomotor nuclei of the monkey. J Comp Neurol 98:449-495.
Wasicky R, Horn AKE, Büttner-Ennever JA (2004) Twitch and non-twitch motoneuron subgroups of the medial rectus muscle in the oculomotor nucleus of monkeys receive different afferent projections. J Comp Neurol 479:117-129.
Wentzel PR, Gerrits NM, Dezeeuw CI (1996) GABAergic and glycinergic inputs to the rabbit oculomotor nucleus with special emphasis on the medial rectus subdivision. Brain Res 707:314-319.
Westphal C (1887) Über einen Fall von chronischer progressiver Lähmung der Augenmuskeln (Ophtalmopregia externa) nebst Beschreibung von Ganglienzellengruppen im Bereiche des Oculomotoriuskerns. Arch Psychiat Nervenheilk 98:846-871.
Xu L, Scheenen WJJM, Roubos EW, Kozicz T (2012) Peptidergic Edinger–Westphal neurons and the energy-dependent stress response. Gen Comp Endocrinol 177:296-304.
Yamaguchi K. 2014. Development of the human oculomotor nuclear complex: Somatic nuclei. Ann Anat 196:394-401.
Yamaguchi K, Honma K (2011) Development of the human trochlear nucleus: A morphometric study. Ann Anat 193:106-111.

Zaki W (1960) The trochlear nerve in man. Study relative to its origin, its intracerebral traject and its structure. Arch Anat Histol Embryol 43:105-120.

Zeeh C, Hess BJ, Horn AKE (2013) Calretinin inputs are confined to motoneurons for upward eye movements in monkey. J Comp Neurol 521:3154-3166.

Zeeh C, Mustari MJ, Hess BJ, Horn AKE (2015) Transmitter inputs to different motoneuron subgroups in the oculomotor and trochlear nucleus in monkey. Front Neuroanat 9. doi.org/10.3389/fnana.2015.00095

ATTACHMENT TO MATERIALS AND METHODS

LABORATORY SOLUTIONS

4% Paraformaldehyd in 0.1M PBS (phosphate buffer), pH 7.4 for 3l

***Solution A:**

1500 ml distilled water heated up to 60°C

+ 120g PFA while stirring

+ 5 drops of 30% NaOH; filtrate

***Solution B:**

1500 ml 0.2M PBS, pH 7.4

Solution A and Solution B were mixed shortly before usage, pH 7,4

Sucrose solution:

10% sucrose solution was prepared by dissolving 50 g Sucrose in 500 ml 0,1M PBS pH 7,4

20% sucrose solution: add 100g sucrose in 500ml 0,1M PBS, pH 7.4

30% sucrose solution: add 150g sucrose to 500 ml 0.1M PBS, pH 7,4

0,1M TBS pH 7,4 (Tris – Puffer)

- 24,2g of Trizma Base
- 17,0g NaCl in 2 l distilled water.

Mixture is stirred and adjusted to ph 7,4 with HCl.

0,05M TBS pH 8 für DAB-Solution

1:1 500 ml 0,1M TBS pH 7,4 + 500 ml distilled water,
adjust pH – value to 8 with NaOH

2% Bovine serum albumin

1 g Albumin bovine in 50 ml 0,1M TBS pH 7,4

0,3 % Triton in 0,1M TBS pH 7,4

1,5 ml in 500 ml 0,1M TBS pH 7,4

Deparaffination and hydration of sections

- 1h	Xylene
- 1x 10 min.	100% alcohol
- 1x 10 min.	96% alcohol
- 1x 10 min.	90% alcohol
- 2x 10 min.	70% alcohol
- 1x 10 min.	Distilled water

Antigen retrieval in water bath (80°C) for paraffin sections

Sections were cooked at a temperature of +80°C for 15 min. in water bath containing sodium citrate puffer (2,94g dissolved in 1000ml distilled water and titrated with 0,1M sodium hydroxide until ph 8,5 - 9,0 is reached), then allowed to cool at room temperature for 15min. After cooling they were immersed shortly in distilled water before rinsing with TBS ph 7,6.

* 0,01M Sodium Citrate Puffer pH 8,8.....**15 min in waterbath at +80°C**
* Allow cooling in Citratpuffer .....for 15 min. at RT
* Rinse in distilled water
* 3x 0,1M TBS pH 7,6.....5 min.
*Immunostaining

Nissl staining

Solution: 0.5g cresyl violet in 100ml distilled water.

70% alcohol for 5 min.

90% alcohol for 5 min.

96% alcohol l for 5 min.

100% alcohol for 5 min.

2x Xylene for 15 min.

100% alcohol for 5 min.

96% alcohol for 5 min.

90% alcohol for 5 min.

70% alcohol for 5 min.

- distilled water for 5 min.

- 0.5% cresyl violet solution for 5 min.

- Sections shortly washed in distilled Water

70% alcohol for 5 min.

90% alcohol for 5 min.

96% alcohol l for 5 min.

100% alcohol for 5 min.

2 x Xylene for 15 min.

Coverslip

Combined immunostaining for ChAT (DAB-Ni, black) and GAD (DAB, brown):

Monoclonal mouse anti- Glutamate Decarboxylase (GAD); Biotrend: GC 3108, Polyclonal goat anti-choline Acetyltransferase = Chemicon, AB144P

Day 1.

* 0,1M TBS pH 7,4.....10 min.

* *Suppression of endogenous peroxidase activity*.....30 min.

1% H_2O_2 in 0,1M TBS

* 3x 0,1M TBS pH 7,4.....each 10 min

* Preincubation.....1h at RT

2% Normal Rabbit Serum + 0,3% Triton in 0,1M TBS pH 7,4

**** Primary antibody***….....2 nights at RT

goat anti-ChAT **1:100** [in **2**% Normal Rabbit Serum/0,3% Triton in 0,1M TBS pH 7,4]

Day 2.

* 3x 0,1M TBS pH 7,4.....each 10 min

* Biotinylated *secondary antibody*:..... 1h at RT

biotinylated rabbit anti-goat 1:200 [In 0,1M TBS + 2% BSA (TBS-BSA)]

* 3x 0,1M TBS pH 7,4.....each 10 min

* *EAP prepared* 30 min before usage.....1h at RT

EAP: Extravidin-Peroxidase 1:1000 [In 0,1M TBS + 2% BSA (TBS-RSA)]

* 2 x 0,1M TBS pH 7,4.....each 10 min

* 1x 0,05M TBS pH 7,6….....10 min

*DAB-Ni Reaction: .....10 min

0,025% DAB + 0,015% H_2O_2 in 0,05M TBS pH 7,6

0,025% DAB = 0,5 ml von 1% DAB-solution in 20ml 0,05M TBS pH 7,6 + 40 mg Ammonium Nickel filtrate, then **20ml 0,025% DAB + 10 µl 30%H_2O_2**

* 3x 0,1M TBS pH 7,4.....each 10 min.

* *Suppression of endogenous peroxidase activity*.....30 min

1% H_2O_2 in 0,1M TBS pH 7,4

* 3x 0,1M TBS pH 7,4.....each 10 min

* Preincubation.....1h at RT

2% Normal Horse Serum + 0,3% Triton in 0,1M TBS pH 7,4

**** 1. Antibody:***….....16-24 hours at RT

Mouse anti-GAD 1:4000 [in **2**% Normal Horse Serum/0,3% Triton in 0,1M TBS pH 7,4]

Day 3.

* 3x 0,1M TBS pH 7,4.....each 10 min

* Biotinylated secondary antibody..... 1h at RT

Biot. horse anti-mouse 1:200 [In 0,1M TBS + 2% BSA (TBS-RSA)]

* 3x 0,1M TBS pH 7,4.....each 10 min

* *EAP* *prepared* 30 min. before usage.....1h at RT

EAP: Extravidin-Peroxidase 1:1000 [in 0,1M TBS + 2% Bovine serum albumin (TBS-BSA)]

* 2 x 0,1M TBS pH 7,4.....each for 10 min

* 1x 0,05M TBS pH 7,6….....10 min

*DAB Reaction: .....10 min

0,025% DAB + 0,015% H_2O_2 in 0,05M TBS pH 7,6

0,025% DAB = 0,5 ml von 1% DAB-solution in 20ml 0,05M TBS pH 7,6

Then**:** 20ml 0,025% DAB + 10 µl 30%H_2O_2

* 3x 0,1M TBS pH 7,4.....each for 10 min

* In [1x 0,1M TBS + 2x distilled water] sections were mounted on object glass

* Allow getting dry at room temperature

* Rinse in distilled water…….…….…….....for 5 min

* In series of ascending alcohol concentration 70, 90, 96, 100%.....each for 5 min

* 3x Xylene……...2x 5 min. and 1x15 min

* Coverslip

Goat anti-ChAT-DAB-Ni + Rabbit anti-Calretinin-DAB

Antibodies:

Polyclonal goat anti-choline Acetyltransferase = Chemicon, AB144P

Polyclonal rabbit anti-Calretinin = SWant, 7699/4

***Sodium Citrate Puffer*:** **0,01M pH 8,5 - 9,0**

- Sodium Citrate 2,94 g
- Distilled water 1000 ml
- Titrated with 0,1M NaOH at pH 8,5 - 9,0

Procedure: * Deparaffination and rehydration of sections

- 1h Xylene
- 1x 10 min. 100% alcohol
- 1x 10 min. 96% alcohol
- 1x 10 min. 90% alcohol
- 2x 10 min. 70% alcohol
- 1x 10 min. Distilled water

* 0,01M Sodium Citrate buffer pH 8,8.....15 min in waterbath at +80°C or in Microwave

* Let cool in Citrate buffer .....for 15 min. at RT

* Rinse shortly in distilled water

* 3x 0,1M TBS pH 7,6..... ….....for 5 min.

Day 1.

* *Suppression of endogenous peroxidase activity* …….....for 30 min

1% H_2O_2 in 0,1M TBS

* 3x 0,1M TBS pH 7,4.....each for 10 min

* *Preinkubation*:.....1hour at RT

5% Normal Horse Serum + 0,3% Triton in 0,1M TBS pH 7,4

**** Primary antibody:***….....48 hours at RT

Goat anti-ChAT **1:100** [in ***5***% Normal Horse Serum + 0,3% Triton in 0,1M TBS pH 7,4]

Day 2.

* 3x 0,1M TBS pH 7,4.....each for 10 min

* Biotinylated *secondary antibody*:.....1h at RT

biot. Horse anti-Goat 1:200 [in 0,1M TBS + 2% Bovine serum albumin (TBS-BSA)]

* 3x 0,1M TBS pH 7,4.....each for 10 min

* *EAP* Extravidin-Peroxidase, *prepared* 30 min before usage.....1h at RT

EAP = Extravidin-Peroxidase 1:1000 [in 0,1M TBS + 2% BSA (TBS-BSA)

* 2 x 0,1M TBS pH 7,4.....each for 10 min

* 1x 0,05M TBS pH 7,6….....for 10 min

*DAB Reaction: .....5 to 10 min

0,025% DAB + 0,015% H_2O_2 in 0,05M TBS pH 7,6

- 0,025% DAB = 0,5 ml von 1% DAB-solution in 20ml 0,05M TBS pH 7,6

+ 40 mg Ammonium Nickel filtrate

then > **20ml 0,025% DAB + 10 µl 30%H_2O_2**

* 3x 0,1M TBS pH 7,4.....each for 10 min

* *Suppression of endogenous peroxidase activity* .....30 min

1% H_2O_2 in 0,1M TBS

* 3x 0,1M TBS pH 7,4.....each for 10 min

* Preincubation:.....1hour at RT

2% Normal Horse Serum + 0,3% Triton in 0,1M TBS pH 7,4

**** Primary antibody:***….....for 48h at RT

rabbit anti-Calretinin 1:2500 [in ***2***% Normal Horse Serum + 0,3% Triton in 0,1M TBS pH 7,4]

Day 3.

* 3x 0,1M TBS pH 7,4.....each for 10 min

* Biotinylated *secondary antibody*:..... 1hour at RT

biot. Horse anti-Rabbit 1:200 [in 0,1M TBS + 2% BSA (TBS-RSA)]

* 3x 0,1M TBS pH 7,4.....each for 10 min

* *EAP*……. *prepared* 30 min before usage.....1hour at RT

EAP = Extravidin-Peroxidase 1:1000 [In 0,1M TBS + 2% BSA (TBS-BSA)]

* 2 x 0,1M TBS pH 7,4.....each for 10 min

* 1x 0,05M TBS pH 7,6-8….. for 10 min

*DAB Reaction: .....for 10 min

0,025% DAB + 0,015% H_2O_2 in 0,05M TBS pH 7,6

- 0,025% DAB = 0,5 ml von 1% DAB-solution in 20ml 0,05M TBS pH 7,6

then > **20ml 0,025% DAB + 10 µl 30%H_2O_2**

* 3x 0,1M TBS pH 7,4.....each for 10 min

* In [2x 0,1M TBS + 1x distilled water] sections mounted on object glass

* Allow drying at room temperature (RT)

* Distilled water…….…….....… for 5 min

* In series of alcohol 70, 90, 96, 100%.....each for 5 min

* 3x Xylene……...……....shortly 2x for 5 min und 1x 15 min

* Coverslip

Gallyas stain

Prior to staining all sections were washed in 70% alcohol for 50min and immersed in 96% alcohol overnight.

Impregnation solution:

475mg of Ammonium nitrate and 500mg of silver nitrate were diluted in 500ml distilled water and titrated with NaOH at PH 7,6

* Production of solutions:

Solution A: 300 ml distilled water + 15 g Natriumcarbonat

Solution B: 300 ml distilled water

+ 600 mg Ammoniumnitrat

+ 600 mg Silbernitrat

+ 3 g Wolframkieselsäure

Solution C: 90 ml B + 0,3 ml Formalin

* Natriumthiosulfat: 200 ml distilled water + 4 g Natriumthiosulfat

* Acetic acid: 995 ml distilled water + 5 ml acetic acid

* Cleaning: 0,5 g Kaliumhexacyanoferrat II + 240 ml distilled water

Pretreatment:

1. Pyridin / aceticanhydrid 2 : 1…….....…60 min
   160 ml 80 ml
2. 3x distilled water ……...……...…… each for 5 min
3. Impregnation at 24°C in darkness (in Water bad on shaker)..... ……60 min
4. Shortly in distilled water
5. 0,5 % acetic acid……...…….10 min
6. 2x distilled water……each for 5 min
7. Mixture: 100 ml solution A + 70 ml solution B + 30 ml solution C = 200 ml
8. Immerse in 0,5 % acetic acid…….shortly
9. 2x distilled water……...…….each for 5 min
10. Clean in Kaliumhexacyanoferrat II……..……..2 min
11. 2x distilled water…….…….each for 5 min
12. 2% Natriumthiosulfat (Fixer)……...……..…1 min
13. Tap water……..…….…….….20 min
14. Dehydrate and coverslip

Single-immunoperoxidase for GAD or non-phosphorylated neurofilaments (NP-NF)

Antibodies:

Mouse monoclonal antibody to Glutamate Decarboxylase (GAD) = Biotrend: GC 3108

Mouse monoclonal antibody non-phosphorylated neurofilaments. Sternberger Monoclonas Incorporated; Cat Nr. SMI 32

Cases: Block II > Group d: Loch: 1,3,5,7,9 > Reaction of free floating sections
Loch: 2,4,6,8 > Reaction of sections on slide
> Group e: Loch: 1,3,5,7,9 > Reaction of free floating sections
Loch: 2,4,6,8 > Reaction of sections on slide

Procedure:

Day 1.

* 0,1M TBS pH 7,4.....10 min

* *Suppression of endogenous peroxidase activity:* .....30 min

1% H_2O_2 in 0,1M TBS pH 7,4

* 3x 0,1M TBS pH 7,4.....each for 10 min

* *Preincubation*:.....1h at RT

2% Normal Horse Serum + 0,3% Triton in 0,1M TBS pH 7,4

**** Incubation: 1. Antibody:***….....for 48h at RT

Mouse anti-GAD **1:4000**

Mouse anti-NP-NF **1:5000**

[in **2**% Normal Horse Serum + 0,3% Triton in 0,1M TBS pH 7,4]

Day 2.

* 3x 0,1M TBS pH 7,4.....each for 10 min

* Biotinylated *2.Antibody*:..... 1h at RT

Biot. Horse anti-Mouse **1:200** [In 0,1M TBS + 2% Bovine serum albumin (TBS-BSA)]

* 3x 0,1M TBS pH 7,4.....each 10 min

* *Extra-Avidin-Peroxidase.....prepare* 30 min earlier.....1h at RT

EAP = Extravidin-Peroxidase 1:1000 [in 0,1M TBS + 2% BSA (TBS-BSA)]

* 2 x 0,1M TBS pH 7,4.....each for 10 min

* 1x 0,05M TBS pH 7,6….....10 min

*DAB reaction: .....10 min

0,025% DAB + 0,015% H_2O_2 in 0,05M TBS pH 7,6

- 0,025% DAB = 0,5 ml von 1% DAB-Solution in 20ml 0,05M TBS pH 7,6

then > **20ml 0,025% DAB + 10 µl 30%H_2O_2**

* 3x 0,1M TBS pH 7,4.....each for 10 min

* Immerge sections in [1x 0,1M TBS + 2x distilled water]

* Allow drying

* Distilled water…….……..5 min

* In alcohol 70, 90, 96, 100%.....each for 5 min

* 3x Xylene…….....……...each for 15 min

* Coverslip

Eidesstattliche Versicherung

Che Ngwa, Emmanuel

Name, Vorname

Ich erkläre hiermit an Eides statt,

dass ich die vorliegende Dissertation mit dem Thema

„Identification of motoneurons innervating individual extraocular muscles within the oculomotor nucleus in human“

selbständig verfasst, mich außer der angegebenen keiner weiteren Hilfsmittel bedient und alle Erkenntnisse, die aus dem Schrifttum ganz oder annähernd übernommen sind, als solche kenntlich gemacht und nach ihrer Herkunft unter Bezeichnung der Fundstelle einzeln nachgewiesen habe.

Ich erkläre des Weiteren, dass die hier vorgelegte Dissertation nicht in gleicher oder in ähnlicher Form bei einer anderen Stelle zur Erlangung eines akademischen Grades eingereicht wurde.

München, den…… ……

Ort, Datum Unterschrift Doktorand

ACKNOWLEDGEMENTS

I am indepted to everyone who in one way or another offered support and encouragement to the completion of this experimental study.

I would like to use this opportunity to specifically express my gratitude and thanks to Prof. Jean Büttner-Ennever for perceptive advices and support throughout my entire studies at the Ludwig-Maximilians-University of Munich. You have been a great inspiration for me and I appreciate so greatly the incredible opportunity I had working in your laboratory. Your broad scientific knowledge, experience, guidance and supervision has extremely been of great help to accomplishing this work and for my academic growth.

Special thanks to Dr. Anja K. Horn-Bochtler, whose teaching skills I have always appreciated. I am so impressed with the alternative views and challenging ideas you offered during experimental procedures and results analysis. In addition I am also grateful for your flexibility, extra hours you spent in the laboratory on my behalf, thorough supervision, valuable instructions and suggestions to different staining techniques implemented.

Particularly I want to thank Ahmed Messoudi for introducing me to laboratory work and for his constant encouragement and support. I want to acknowledge how I benefited from his experience as a Laboratory technician and for increasing my efficiency in staining techniques.

I am also truly grateful to Rita Büttner, Karoline Fackelmann, Christina Schulze, Christina Glombik and Christopher Adamczyk for welcoming me into the oculomotor group and for creating a suitable atmosphere for academic development.

I also want to cordially thank my family especially my sister Rebecca Ngaling for her incredible and endless love, support, and encouragement as well as Sandrine Che Ngwa for her love, valuable ideas and suggestions.

Last but not the least, great thanks to Stefan Bertog MD and to all my friends for their great support.